

1 **INDISIM-Denitrification, an individual-based model for study the denitrification process**

2

3 Pablo Araujo-Granda^{1*}, Anna Gras², Marta Ginovart³, Vincent Moulton⁴

4

5 ¹ Chemical Engineering Faculty, Universidad Central del Ecuador, Ciudad Universitaria, Ritter y Bolivia, P.O.Box. 17-
6 01-3972, Quito - Ecuador; e-mail: paaraujo@uce.edu.ec

7 ² Department of Agri-Food Engineering and Biotechnology, Universitat Politècnica de Catalunya, Edifici D4, Esteve
8 Terradas 8, 08860 Castelldefels, Barcelona - Spain; telephone: (34) 935521224; e-mail: anna.gras@upc.edu

9 ³ Department of Mathematics, Universitat Politècnica de Catalunya, Edifici D4, Esteve Terradas 8, 08860 Castelldefels,
10 Barcelona - Spain; telephone: (34) 935521133; e-mail: marta.ginovart@upc.edu

11 ⁴ School of Computing Sciences, University of East Anglia, Norwich Research Park, Norwich NR4 7TJ - United
12 Kingdom; telephone: (44) 1603 592607; e-mail: v.moulton@uea.ac.uk

13

14 * Corresponding author: e-mail: pablo@araujo.ec or paaraujo@uce.edu.ec, telephone: (593) 999220560

15

16 **Abstract**

17 Denitrification is one of the key processes of the global nitrogen (N) cycle driven by bacteria. It has been widely known
18 for more than one hundred years as a process by which the biogeochemical N-cycle is balanced. To study this process,
19 we develop an individual-based model called INDISIM-Denitrification. The model embeds a thermodynamic model for
20 bacterial yield prediction inside the individual-based model INDISIM and is designed to simulate in aerobic and anaerobic
21 conditions the cell growth kinetics of denitrifying bacteria. INDISIM-Denitrification simulates a bioreactor that contains
22 a culture medium with succinate as a carbon source, ammonium as nitrogen source and various electron acceptors. To
23 implement INDISIM-Denitrification, the individual-based model INDISIM was used to give sub-models for nutrient
24 uptake, stirring and reproduction cycle. Using a thermodynamic approach, the denitrification pathway, cellular
25 maintenance and individual mass degradation were modelled using microbial metabolic reactions. These equations are
26 the basis of the sub-models for metabolic maintenance, individual mass synthesis and reducing internal cytotoxic
27 products. The model was implemented in the open-access platform NetLogo. INDISIM-Denitrification is validated using
28 a set of experimental data of two denitrifying bacteria in two different experimental conditions. This provides an
29 interactive tool to study the denitrification process carried out by any denitrifying bacterium since INDISIM-
30 Denitrification allows changes in the microbial empirical formula and in the energy-transfer-efficiency used to represent
31 the metabolic pathways involved in the denitrification process. The simulator can be obtained from the authors on request.

32
33 **Keywords:** denitrification, bacterial yield prediction, individual-based model, Thermodynamic Electron Equivalents
34 Model, NetLogo, INDISIM.

35

36 1. Introduction

37 For the past decades, scientists have experienced huge interest in crossing the frontiers between different disciplines such
38 as mathematics, biology, chemistry, thermodynamics and modelling, among others. Thus, this is a study of microbial
39 metabolism in the framework of non-equilibrium thermodynamics and individual-based modelling, both concepts being
40 applied to bacterial denitrification systems evolving in a bioreactor.

41 Denitrification is the dissimilatory reduction of nitrate (NO_3^-) to (mainly) dinitrogen gas (N_2) by bacteria. Hence, one or
42 both of the ionic nitrogen oxides, NO_3^- and nitrite (NO_2^-), can be reduced to the gaseous oxides, nitric oxide (NO) and
43 nitrous oxide (N_2O), which consequently may also be reduced to N_2 [1, 2]. A complete denitrification pathway is defined
44 as the assemblage of four subsequent reactions: $\text{NO}_3^- \rightarrow \text{NO}_2^- \rightarrow \text{NO} \rightarrow \text{N}_2\text{O} \rightarrow \text{N}_2$ [1, 3].

45 Denitrification has been described, studied and investigated over the last one hundred years [4] at many levels, ranging
46 through gene expression of the enzymes involved in the process [5–10], describing microbial metabolic pathways [11–
47 14], measuring global N-oxides flux [15–17], evaluating the impact of metal concentrations in the soil on the expression
48 of enzymes in different species of denitrifying bacteria [18–20], contributing to wastewater treatments as well as other
49 biological systems [21, 22], within mathematical modeling [23–28] and, in individual-based models [29–32].

50 Interest in denitrification is motivated by several key factors. First, it is a fundamental process in wastewater treatment to
51 reduce NO_3^- excess and stimulate carbon removal in anoxic conditions [33]. Second, it contributes to nitrous N_2O and/or
52 NO emissions when denitrifying bacteria do not complete the metabolic pathway implicated, which is involved in
53 atmospheric phenomena like global warming and ozone damage [34, 35]. Third, it is the mechanism by which the global
54 nitrogen cycle is balanced [36].

55 Denitrification is a process driven by bacteria species with a genetic capacity for denitrification; they are classified as
56 facultative aerobes. The denitrification pathway is common among several microbial species: *Pseudomonas*,
57 *Achromobacter* (*Alcaligenes*) [37], *Paracoccus*, *Thiobacillus*, *Bacillus*, *Halobacterium*, *Chromobacterium*,
58 *Hyphomicrobium*, in addition to some species of *Moraxella* that are also able to denitrify [22, 36]. Most of them are
59 commonly found in soils, sediments, surface and ground waters, and wastewater treatment plants [33]. Denitrifying
60 bacteria are able to use N-oxides as electron acceptors (e-acceptors) instead of oxygen (O_2), by electron transport chains
61 similar to the ones used in aerobic respiration [6]. This means that they shift to NO_3^- or NO_2^- or NO or N_2O respiration
62 when O_2 becomes limiting [22].

63 There are a wide range of environmental factors that control the complex regulatory network involved in bacterial
64 denitrification. These include low O_2 concentration and the availability of e-acceptors (NO_3^- , NO_2^- , NO, N_2O) and C-
65 sources as electron donors (e-donors) in the local environment where the bacteria develop [1]. Further, there is some

66 evidence that the denitrifying bacteria have the ability to reduce their own biomass to avoid accumulation of cytotoxic
67 intermediate products (N_2O and/or NO) and complete the denitrification pathway and maximize energy conservation [11,
68 22]. In addition, if any of the key factors that control the denitrification pathway provoke an interruption of the process,
69 then cytotoxic gases (N_2O and/or NO) are released to the medium. This can be viewed as a negative environmental
70 consequence of denitrification since NO participates in photochemical reactions to produce tropospheric ozone, a
71 greenhouse gas. The soil emissions of NO to the atmosphere have been measured and modeled in order to control its
72 production [15, 23]. N_2O is a potent greenhouse gas and dominant ozone-depleting substance [9, 18, 19, 36]. Further,
73 these gases have bacterial cytotoxic properties [5, 20] such as essential cellular cofactor inactivation of B12-dependent
74 enzymes [7, 38], loss of cell division and viability [1, 4].

75 To study and analyze a microbial system, it is crucial to recognize the *structured* nature of each cell and the *segregation*
76 of the culture into individual units that may differ from each other [39]. Therefore, it is crucial to carefully select the
77 modeling approach.

78 The modelling approach traditionally used in biological fields, is an approach to understanding population level, where
79 the population parameters are time-dependent and modified directly using the model's equations [40]. Models built at a
80 population level of description are a particular type of System-based Model (SBM) [41]. They consider variables that
81 characterize the population and the set of laws governing it. These rules are usually formalized with differential equations,
82 which are ultimately based on assumptions regarding the behavior of the individuals. SBMs consist in defining the
83 relevant variables of the system and proposing a set of rules governing them, applying these rules, i.e. solving the
84 equations, and assessing the validity of the model through the comparison of its results with experimental observations
85 [42]. Some of the applications of these models are predictive microbiology in food and control of fermentation processes
86 [43], optimization of microbial cultures and antibiotics production in the pharmaceutical industry [44], waste control and
87 water treatment [21], or the study of microbial ecology and evolution of population diversity in wild and artificial
88 ecosystems [33]. Population models are based on assumptions about the individual behavior of microbes, and they
89 therefore also raise new questions regarding microbial physiology and cellular models [45, 46].

90 Individual-based modeling is implemented and used in many scientific contexts, such as biological, chemical,
91 biotechnological, ecological, among others [40, 47]. In this type of modeling, the interactions of the agents (individuals
92 and/or collective entities) with their environment are simulated and the population-level behavior is an emergent property
93 [48]. The IBM of microbes is called the "microbial individual-based model" (μIBM) [49]. Such models provide some
94 advantages over the population-level approaches commonly used to model microbes' processes since: (a) they describe
95 the system evolution as a whole by establishing behavior-rules for the microbes and their relations; (b) they can reproduce
96 system variability because they admit the introduction of randomness and specific characteristics for the microbes; (c)

97 they take into account the individual adaptive behavior to the local environmental conditions; (d) they have the capability
98 to resolve population heterogeneity (intra-population variability) to deal with complete life cycles, and (e) they represent
99 the individual adaptive behavior to deal with internal and external conditions that changing over the time [48, 50, 51].
100 Also IBMs have the ability to link mechanisms at the individual level to population level behavior (emergence), and they
101 are very convenient to tackle the inapplicability of the continuum hypothesis [46, 52]. Therefore, the individuals and their
102 internal differences and actions are better represented with a μ IBM, in which the population behavior is the consequence
103 of a set of microbes growing and interacting with the local environment [42, 47, 49, 52–54]. However, the potential of
104 IBMs has a cost. They are more complicated structurally than analytical models, they must be implemented and executed
105 in computers with determinate computing capabilities (modelling large-scale systems), the lack of individual-based data
106 is sometimes crucial for their progress, besides they present some difficulties at the time of analysis, understanding and
107 communicating [55]. To mitigate some of these problems there has been established the ODD protocol which stands for
108 Overview, Design and Details as the universal way used by the scientific community for presenting and describing their
109 IBMs [40, 47, 48, 56]. The use of specific programming environments to implement these computational models
110 facilitates their use [55, 57], which along with computer processing tools and statistical analysis of data provides
111 parameter estimation and the corresponding sensitivity analysis. These facilities make the methodology of discrete
112 modelling based on the individual a valid and attractive option for study of microbial systems, increasing its presence in
113 academic [58–61] and scientific fields [56, 62–65].

114 INDISIM is an individual-based discrete simulation model developed to study bacterial cultures [66]. This model has
115 been used as the core for other models such as INDISIM-SOM [67, 68] and INDISIM-SOM-NL [69], INDISIM-YEAST
116 [70], INDISIM-COMP [71], and INDISIM-*Saccha* [53] to model: the soil organic matter dynamics, yeast fermentation,
117 multi-species composting, and the dynamics of *Saccharomyces cerevisiae* in anaerobic cultures, respectively.

118 Commonly, the biomass volumetric productivity and the macro-molecular composition of the cells are studied with
119 regards to the potential production of the cells in response to their environment within the cultivation system [72].
120 According to the principles of the thermodynamics of non-equilibrium systems, a microorganism keeps alive by taking
121 energy from its environment to maintain its structures and functions [73].

122 Taking into account this perspective, in the past few decades, several approaches in bio-thermodynamics, non-equilibrium
123 thermodynamics, and network thermodynamics have been developed and reported to study and describe a macroscopic
124 growth model for biomass yield prediction and cellular bioenergetics [22, 72, 74–88]. These approaches can be useful in
125 the calculation of: (a) the complete growth stoichiometry, (b) the maintenance coefficients and maximal growth yields,
126 (c) the limit to growth yield posed by the second thermodynamic law, (d) the chemical-oxygen-demand-based growth
127 yields, and (e) the maximal product yields in aerobic and anaerobic metabolism. Therefore, these thermodynamic

128 approaches aim to represent all reactions that occur in the microorganisms using a set of microbial metabolic reactions
129 (MMRs) [30, 31]

130 Using INDISIM [66] as a core model, we developed a model called INDISIM-Paracoccus [31] which is the first μ IBM
131 to use thermodynamics concepts to write the MMRs for cellular maintenance and individual mass production. It was
132 designed to investigate the order of preference in the use of various e-acceptors in the denitrification process driven by
133 *Paracoccus denitrificans*. With that model, we were able to fix the sequence order of the reduction of NO_3^- semi reactions
134 along the denitrification and obtained a set of model parameter values to get a reasonably good fit of the simulation
135 outputs to experimental data. INDISIM-Paracoccus had two main limitations, one was that it is only useful for one species
136 of bacteria, the *P. denitrificans*, while there are many other bacteria that are able to denitrify. The second limitation was
137 that some of the simulation outputs related to the cytotoxic gas nitrous oxide in the electron-donor limited and electron-
138 acceptor limited experiments were not predicted accurately enough when compared with experimental data [32]. This
139 current work aims to improve INDISIM-Paracoccus in order to overcome these limitations and provide it with a greater
140 use and predictive capacity.

141 We develop an μ IBM that is called INDISIM-Denitrification (Fig. 1) to deal with the dynamics of any denitrifying
142 bacterium in aerobic and anaerobic conditions, including a thermodynamic model based on bioenergetics efficiency to
143 describe the microbial metabolism. In particular, (a) we select the common pathways expressed in any denitrifying
144 bacterium and represent them using a thermodynamic approach as a set of MMRs (which are central to the formulation
145 of the metabolic sub-models inside of the μ IBM developed), (b) we include into these MMRs the elemental composition
146 of the microbial cells using a generic empirical formula that considers the molar relationship between the four main
147 elements (C, H, O and N), (c) we design and parameterize behavior-rules plausible for any denitrifying bacterium with
148 three main metabolic purposes: cellular maintenance, mass synthesis and individual mass degradation to reduce internal
149 cytotoxic products; (d) we simulate a bioreactor that contains a culture medium where denitrifying bacteria develop and
150 grow; (e) we implement the model on the open-access platform NetLogo presenting an μ IBM simulator; and (f) we test
151 the adequacy of the model using a set of experimental data for the denitrifying bacteria *P. denitrificans* and
152 *Achromobacter xylosoxidans* published by Felgate et al. (2012). The use of a broader set of experimental data of two
153 different denitrifying bacteria *P. denitrificans* and *A. xylosoxidans* leads to a better agreement to *P. denitrificans* data than
154 previously obtained and open the possibility to deal with a new bacterium (*A. xylosoxidans*).

155 2. Materials and methods

156 2.1 Thermodynamic approach

157 The Thermodynamic Electron Equivalents Model (TEEM) is designed for bacterial yield prediction [22, 74, 81, 88–90].
158 TEEM is based on terms of the Gibbs free energy involved in the overall metabolic process and in how the energy between
159 catabolism and anabolism is coupled using a term of energy-transfer-efficiency (ε). TEEM has two versions, the first one,
160 TEEM1 [22] considers a realistic formulation of the anabolic reaction taking into account different N-sources such as
161 NH_4^+ , NO_3^- , NO_2^- and N_2 , and a complete explanation of ε between catabolism and anabolism. The second version,
162 TEEM2 [74] complements TEEM1 because it considers oxygenase reactions involved and the aerobic heterotrophic
163 oxidation of C1 organic compounds.

164 For the use of any version of TEEM, first, we need to identify the e-donor(s) (usually the C-source) and the e-acceptor(s)
165 and write reduction-half-reactions for each one of them. Second, it is necessary to establish the N-source for biomass
166 synthesis and the empirical chemical formula that will represent the cells.

167 According to TEEM, to write the energy equation (Re) which represents the microbial catabolism, we need to combine
168 the reduction-half-reaction of an e-donor (Rd) with the reduction-half-reaction of an e-acceptor (Ra). Once the catabolic
169 process is represented by the Re equation, it is necessary to write the reaction for the cellular synthesis (Rs) that will
170 represent the microbial anabolism. To do this, we need to combine the reduction-half-reaction of Rd with the cell synthesis
171 half-reaction (Rc). For Rc we have to write and balance a hypothetical half-reaction that consider as reactants: The N-
172 source (NH_4^+ , NO_3^- , NO_2^- or N_2), CO_2 and HCO_3^- , and as products: water and the microbial mass represented by an
173 empirical chemical formula of cells ($\text{C}_n\text{H}_a\text{O}_b\text{N}_c$). This empirical chemical formula considers only the four basic elements:
174 Carbon (n), Hydrogen (a), Oxygen (b) and Nitrogen (c). To estimate the Gibbs free energy of this half-reaction (Rc),
175 TEEM uses a value of 3.33 KJ per gram cells [88] which is related to one generic microbial cell composition ($\text{C}_5\text{H}_7\text{O}_2\text{N}$).
176 To couple the energy from catabolism to anabolism, TEEM establishes a relation with the electrons involved. The
177 electrons that come from the e-donor are divided in two parts, a fraction (fe^o) is transferred to the e-acceptor to generate
178 energy (catabolism) and another fraction (fs^o) is transferred to the N-source for cell synthesis (anabolism). TEEM
179 calculates the relationship between fe^o and fs^o using: (a) Gibbs standard free energy of Rd , Ra and Rc , (b) other Gibbs
180 standard free energy terms related to C1 carbon source and oxygenase's enzymes, and (c) a term for energy-transfer
181 efficiency (ε). This term is included because TEEM assumes that a fraction of thermodynamic free energy is lost at each
182 transfer energy between catabolism and anabolism. TEEM's developer [22, 74] used an extensive amount of information
183 provided by several authors, Heijnen and Van Dijken, 1992; VanBriesen and Rittmann, 2000; VanBriesen, 2002; Xiao
184 and VanBriesen, 2008, to calibrate and determine the best-fit energy-transfer-efficiency (ε) for the TEEM model.

185 Therefore, using TEEM we can get the complete chemical and energetic stoichiometry of microbial growth represented
186 by a MMR. In this study, we will represent metabolic pathways as a set of MMRs using TEEM2 and use them as the
187 basis of the behavior-rules (such as individual cellular maintenance or individual mass synthesis or individual mass
188 degradation to reduce cytotoxic products) for each bacteria of the virtual system, and we assume the ε value as an
189 individual value [30].

190 2.2 Experimental data

191 To study into a bioreactor the denitrification process, the experimental assays were designed to breed and develop bacteria
192 in a bioreactor under two different conditions: one first stage in a batch culture (from 0 to 24 h) during the aerobic phase,
193 and the second one in a continuous culture (from 24 to 120 h) during the anaerobic phase. Under these bioreactors
194 procedures two experiments were performed with two different bacterial species by Felgate et al. (2012): (a) the reservoir
195 medium feed contained 20 mM NO_3^- , 5 mM succinate and 10 mM NH_4^+ which was designed to achieve an e-donor limited
196 with e-acceptor sufficient during the steady state and is designed as *succinate-limited/ NO_3^- -sufficient* (Experiment E1),
197 and (b) the reservoir medium feed contained 5 mM NO_3^- , 20 mM succinate and 10 mM NH_4^+ to achieve an e-donor
198 sufficient with e-acceptor limited during the steady state and is designed as *succinate-sufficient/ NO_3^- -limited* (Experiment
199 E2). The data for the time evolutions of dry mass (biomass), NO_3^- , NO_2^- and N_2O were collected from 0 to 120 h, according
200 to the experimental procedure presented in Felgate et al. (2012) that utilizes two different denitrifying bacteria, the *P.*
201 *denitrificans* and *A. xylosoxidans*. With INDISIM-Denitrification we will carry on virtual experiments to reproduce the
202 behavior of both bacteria growing in both media.

203 2.3 Programming environment

204 INDISIM-Denitrification is implemented in the widely used, free and open source platform NetLogo (Fig. 2), a multi-
205 agent programming language to modeling environment for simulating natural phenomena [57]. This provides full access
206 to the simulation model, including a graphical user interface and the model's source code. Given NetLogo's rather flat
207 learning curve and comprehensive documentation [40], users without extensive modeling experience can also modify the
208 code and, thus, investigate alternative mechanisms or adapt certain processes according to other approaches (e.g.
209 introducing variations in the biomass empirical chemical formula of bacteria).

210 2.4 Model analysis

211 To assess the validity of the model, after the first visual techniques with subjective assessment, we carried out numerical
212 validation techniques that provide a quantification of the difference (or similarity) between observed and simulated values.
213 The goal is to find ranges of values for the model parameters' that make it possible to roughly reproduce the evolution of

214 a set of focus variables observed in the two trials using the experimental data for the two bacteria, *P. denitrificans* and *A.*
215 *xylooxidans* [18].

216 In order to compare the simulation results with the experimental data we used the geometric reliability index (GRI) values,
217 a statistical method to determine the reliability of a model [93]. This index can deal with precise notions of model
218 accuracy; therefore, its value indicates how closely the simulation results match the experimental ones. For models with
219 simulation results reasonably close to experimental observations this GRI shows a resulting factor of 1 to 3, with 1
220 corresponding to 100% accuracy. The interpretation of GRI is that the simulation is accurate within a multiplicative factor,
221 e.g. with a GRI value equal to 1.32, this means that the simulated values fall between 1/1.32 and 1.32 times the
222 corresponding experimental values [94].

223 The combination of the use of multiple deviance measures with visual inspection in the exploratory data analysis can help
224 to identify deficiencies and capabilities of the model developed. To assess whether a certain combination of model
225 parameter values leads to acceptable model output, we include the GRI calculation within the main code of the simulator
226 for the evolution of four variables: microbial biomass (dry mass), NO_3^- , NO_2^- and N_2O , controlled for each one of the two
227 scenarios (Experiments E1 and E2) and for the two denitrifying bacteria tested (*P. denitrificans* and *A. xylooxidans*).

228 The software tool “BehaviorSpace” incorporated in NetLogo was used for running simulation experiments varying
229 parameters values and writing model outputs data to files to be statistically analyzed. Each simulation is replicated three
230 times.

231 **3. Results and discussion**

232 INDISIM-Denitrification model was developed to reproduce a bioreactor experimental protocol for the denitrification
233 process carried out by denitrifying bacteria growing in batch and continuous culture, in aerobic and anaerobic growing
234 conditions. To describe our model we use the ODD protocol (“Overview, Design concepts, and Details”), which helps to
235 ensure that the model description is complete [40, 47, 95]. The complete and detailed description of this model can be
236 found in the Supplementary material ‘ODD of the model INDISIM-Denitrification’. In this section only, the new features
237 of the model in relation to INDISIM-Paracoccus are highlighted.

238 **3.1. Microbial metabolic reactions**

239 The reduction of cytotoxic products as a result of anaerobic metabolism through the individual-mass degradation has been
240 added to individual metabolism, joint with the cellular maintenance and the individual-mass synthesis (Supplementary
241 material). It seems feasible that in natural conditions when the level of cytotoxic compounds in the media is high then the
242 microorganisms follow different biological strategies to survive. We have assumed and modelled that the individual can

243 use its own mass as an e-donor and the NO and/or N₂O as e-acceptor to keep the levels of those products below toxic
244 concentrations. We consider a degradation coefficient (h⁻¹) to establish the amount of individual mass that is used to reduce
245 cytotoxic products, its value is depending on the bacterial species. The individual mass decreases according to this
246 quantity.

247 To raise the model to a wider number of bacterial species capable to denitrify, we considered the microbial biomass
248 composition represented by the elemental formula of C_nH_aO_bN_c, being the sub index the elemental molar relation. The
249 molar relation can be modified in the computational model by the user according to the microorganism to simulate and
250 in consequence the thermodynamic calculations using TEEM2 have been generalized.

251 To derive the MMRs required for the individual behavior-rule for cellular maintenance, it is necessary to model the energy
252 reactions for aerobic and anaerobic metabolism. We considered the reaction between succinate (which is always the e-
253 donor) and O₂ (as e-acceptor) for the aerobic phase, while for the anaerobic phase; the e-acceptor is an N-oxide. We used
254 the inorganic half-reactions for *Rd* and various *Ra* shown in Rittmann and McCarty, (2001) to write the energy reactions
255 (*Re*) shown in Table 1. With these energy reactions and an appropriate maintenance requirement (gCdonor gCmic⁻¹ h⁻¹),
256 we designed the individual rule for cellular maintenance.

257 For individual-mass synthesis, it is necessary to model the metabolic pathways for aerobic and anaerobic conditions for
258 a general denitrifying bacterium and they are translated into a set of MMRs. To incorporate this in the model we took a
259 rough approximation to the microbial biomass represented by an empirical chemical formula of cells (C_nH_aO_bN_c), which
260 is written only with the molar relationship of the four main elements, *n* for carbon, *a* for hydrogen, *b* for oxygen and *c* for
261 nitrogen. We consider that the microorganism increases its individual-mass when it executes any of the reactions
262 described as a set of MMRs (Table 2), in aerobic phase executes aerobic respiration (Reaction I) and dissimilatory nitrate
263 reduction IV (Reaction II), and in anaerobic phase executes denitrification (Reactions III to VI) [12]. To formulate these
264 reactions and calculate the corresponding stoichiometric coefficients we used the TEEM methodology [74]. In all
265 reactions succinate is the universal *Rd* and C-source, NH₄⁺ is the universal N-source (*Rc*) for cell synthesis and the
266 nutrients used as *Ra* are different, in aerobic conditions they are O₂ and NO₃⁻ and in anaerobic conditions they are NO₃⁻,
267 NO₂⁻, NO and N₂O (Table 2).

268 For the individual mass degradation, to reduce internal cytotoxic products, we write the half-reaction where the biomass
269 is an e-donor which can be coupled with e-acceptor half-reaction to write the stoichiometry reaction (Table 3). With
270 TEEM2 methodology all reactions, for cellular maintenance (Table 1), for individual-mass synthesis (Table 2) and for
271 individual mass degradation (Table 3) are balanced for mass and energy.

272 3.2 Parametrization and sensitivity analysis

273 INDISIM-Denitrification has the capability to work with any denitrifying bacterium. To test the performance of
274 INDISIM-Denitrification we used experimental data published for two different denitrifying bacteria, *P. denitrificans* and
275 *A. xylosoxidans*, and compared them with the simulation results obtained with the NetLogo implementation of our model.
276 To set up the thermodynamic model, we first used the empirical chemical formula ($C_3H_{5.4}O_{1.45}N_{0.75}$) for the denitrifying
277 bacterium *P. denitrificans* published by van Verseveld et al., (1983, 1979, 1977). Taking into account the coefficients n ,
278 a , b and c , the molar relationship between carbon, hydrogen, oxygen and nitrogen, are 3, 5.4, 1.45 and 0.75, respectively,
279 and the information provided by Table 2 and Table 3. The stoichiometric coefficients for each MMR related to individual-
280 mass synthesis (Table 4) and to individual-mass degradation to reduce cytotoxic products (Table 5) were obtained
281 applying TEEM2 [30, 46] with an assigned ε value in the range proposed for McCarty (1971, 2007) and Rittmann and
282 McCarty (2001) (see supplementary material to detailed calculations).

283 To represent the microbial biomass of *A. xylosoxidans* through an empirical chemical formula we adopted $C_5H_9O_{2.5}N$ [26,
284 80, 83] and used the information provided by Table 2 and Table 3, the stoichiometric coefficients for each MMRs related
285 to individual-mass synthesis (Table 6) and to individual-mass degradation to reduce cytotoxic products (Table 7) were
286 obtained operating with TEEM2 [46], using a different assigned ε value for each reaction in the range proposed by
287 McCarty (2007) and Xiao and VanBriesen (2008).

288 The model implementation in NetLogo allows the user to quickly and easily change many parameter's values involved,
289 and specifically, in this new simulator:

290 (a) The molar relationship between the elements of the biomass empirical formula (C, H, O and N), with which the
291 NetLogo simulator immediately recalculates all of the stoichiometric coefficients for the set of MMRs.

292 (b) The bacteria size, allowing the spherical equivalent diameter (expressed in μm) for the smallest and largest bacteria,
293 where in all cases the bacterium is considered to be spherical shape. In the case of *P. denitrificans* the smallest individual
294 represents a bacterium with a diameter of $\sim 0.5 \mu\text{m}$ and the largest one a bacterium with a diameter of $\sim 0.9 \mu\text{m}$. In the
295 case of *A. xylosoxidans* the smallest individual represents a bacterium with a spherical equivalent diameter of $\sim 0.63 \mu\text{m}$
296 and the largest one a bacterium with a spherical equivalent diameter of $\sim 1.40 \mu\text{m}$.

297 (c) The maximum population growth rate (μ_{max} which is expressed in h^{-1}), a parameter which is used to estimate the
298 individual maximum uptake-rates (ui) which are calculated adding the maintenance and growth requirements according
299 the stoichiometric coefficients of the MMRs. van Verseveld et al. (1983) reported for *P. denitrificans* a growth rate value
300 equal to 0.418 h^{-1} , which was obtained in the change from a culture growing in anaerobic NO_3^- -limited conditions to
301 aerobic succinate-limited conditions. In the case of *A. xylosoxidans* a value equal to 0.25 h^{-1} is reported, which was
302 obtained when the bacterium grew over 6-carbon compounds in aerobic conditions [99]. With this information, the

303 simulator recalculates the maximum uptake reference value to all nutrients considered in the virtual system. Using these
304 values and performing calculations with the stoichiometric coefficients of each MMRs adjusted by TEEM2 (Table 4 and
305 Table 6), we obtained the maximum uptake-rate for each nutrient and bacteria. Taking into account the maximum uptake-
306 rate for each nutrient and bacteria, we established the values for the sensitivity analysis performed for this parameter
307 (Table 8 and Table 9).

308 (d) The maintenance coefficient ($\text{gC}_{\text{donor}} \text{gC}_{\text{mic}}^{-1} \text{h}^{-1}$), a parameter which is used in the aerobic and anaerobic growth
309 phases of the denitrifying bacteria. In the case of cellular maintenance, Gras et al. (2011) consider an appropriate
310 maintenance requirement for soil heterotrophic microorganisms of $0.002 (\text{gC}_{\text{donor}} \text{gC}_{\text{mic}}^{-1} \text{h}^{-1})$, which was assumed in
311 INDISIM-Paracoccus [31] for the aerobic phase. This is different in the implementation of INDISIM-Denitrification, due
312 to that the model considering a unique parameter for the cellular maintenance coefficient ($\text{gC}_{\text{donor}} \text{gC}_{\text{mic}}^{-1} \text{h}^{-1}$) in both
313 aerobic and anaerobic phase.

314 (e) The mass degradation coefficient (h^{-1}), another individual parameter related to the individual mass, which was
315 introduced for the anaerobic phase only. In Table 10 we show the tested values for cellular maintenance and individual
316 mass degradation parameters: these ranges of values will be the same for both bacteria.

317 To start the calibration and sensitivity analysis process, we combined the values from Table 8 and Table 9 using a full
318 factorial design for each species of bacteria and each virtual experiment (E1, E2), and after that, we combined the values
319 from Table 10 in a full factorial design for the cellular maintenance and mass degradation coefficients.

320 To assess whether a certain combination of model parameter values leads to acceptable model output, we calculated GRI
321 value for four variables: microbial biomass (drymass), NO_3 , NO_2^- and N_2O , controlled for both scenarios (Experiments
322 E1 and E2) and for both denitrifying bacteria *P. denitrificans* and *A. Xylooxidans*.

323 The simulation and experimental mean values of the three replications performed are presented with their corresponding
324 standard errors in the following graphical representations. We established multiple fitting criteria using the model's
325 parameters: uptake-rate for all nutrients involved, cellular maintenance rate and, mass degradation coefficient, with the
326 experimental data of Felgate et al. (2012). The essential idea is to find a value or a range of values for these parameters
327 that make it possible to roughly reproduce the evolution of a set of patterns observed in the two experiments and for both
328 bacteria species. All full factorial designs were executed using the tool "BehaviorSpace" included in NetLogo, a task that
329 was facilitated due to the simulator including in its code the complete experimental data set to calculate GRI. Each
330 simulation result was compared to the experimental values and the GRI for each one was calculated. We selected the
331 combination of the parameters with minimum GRI value to declare the best fit of INDISM-Denitrification.

332 3.3 Simulation outputs

333 In order to verify our model implementation, we checked several features to ensure its accurate quantification of the
334 conceptual model. For instance, one of the main checks was to verify that the simulator accomplished mass-balances for
335 C and N, which ensures that the chemical reactions and the bioreactor inputs/outputs are accurately implemented, and the
336 simulator works as is expected. We also tested that the individuals were able to carry out all of the reactions in different
337 media compositions. In addition, we systematically investigated internal model logic and behaviors by collecting global
338 and individual data through the simulation, which were numerically and visually tested (Fig. 2).

339 The outputs of the model (Fig. 2) are: (a) the concentration ($\text{mmol}\cdot\text{l}^{-1}$ or $\text{umol}\cdot\text{l}^{-1}$) of each culture medium component
340 (succinate, NH_4^+ , O_2 , NO_3^- , CO_2 , HCO_3^- , NO_2^- , NO , N_2O and N_2), (b) microbial biomass ($\text{mg}\cdot\text{ml}^{-1}$), (c) the population
341 mass distribution, (d) a graphical view to show the frequency of use of each metabolic reaction, (e) all MMRs written
342 using TEEM for any denitrifying bacteria, and (f) GRI's values for the time evolution of system variables, microbial
343 biomass (dry mass), NO_3^- , NO_2^- and N_2O . The outputs of the model that are compared with experimental data are shown
344 in the figures 3 to 6, in these figures the experimental data are drawn with means of the replicates and their standard
345 errors, and the simulation results are drawn with a sequence of dots, each dot represents the mean of the replicates of the
346 model in each step time.

347 3.3.1 Simulations for *P. denitrificans*

348 INDISIM-Denitrification was used to simulate the growth and behavior of the *P. denitrificans* in a bioreactor which works
349 in aerobic conditions (batch culture) and in anaerobic conditions (continuous culture) in accordance with the experiments
350 E1 and E2 and experimental protocols published by Felgate et al. (2012). The set of individual and environmental
351 parameter values that generate model outputs with acceptable GRI coefficient are shown in Table 11. In figure 3 and
352 figure 4, we present the outputs assessed for the bacterium *P. denitrificans*, namely the drymass, NO_3^- , NO_2^- and N_2O
353 time evolutions for the two experiments succinate-limited/ NO_3^- -sufficient – E1 (Fig. 3) and succinate-sufficient/ NO_3^- -
354 limited – E2 (Fig. 4) with the GRI score obtained in the statistical analysis.

355 According to the magnitude of the GRI coefficient, the results of the simulated experiment E1, succinate-limited/ NO_3^- -
356 sufficient, are accurate to the experimental results for drymass, NO_3^- , NO_2^- and N_2O evolutions. The experimental data
357 suggest that the culture achieved the steady state 40 hours from the start; the effect of moving from aerobic to anaerobic
358 phase, is appreciable on the GRI values for NO_2^- (Fig. 3-C) and N_2O time evolution (Fig. 3-D), the highest values obtained
359 are for E1, but still adequate. Furthermore, we consider that the results on figures 3-C and 3-D are due to the stochastic
360 nature of the parameter related with the behavior-rule of the individual-mass degradation to reduce cytotoxic products are
361 executed, observing these results we confirm that our model has the necessary stochasticity that an IBM must have.

362 The lowest value obtained for GRI corresponds to the drymass temporal evolution (Fig. 3-A), which confirms that the
363 thermodynamic approach used to represent the metabolic pathways was properly selected.

364 The results obtained for the simulated experiment E2, succinate-sufficient/NO₃⁻-limited, are close to the experimental
365 result for drymass evolution (Fig. 4-A). On the other hand, the GRI scores for NO₃⁻, NO₂⁻ and N₂O evolutions in E2 (Fig.
366 4-B, Fig. 4-C and Fig. 4-D) are outside of the required GRI range, which suggests a rough adequacy of the model in the
367 experiment e-donor-sufficient/e-acceptor-limited.

368 An explanation for this fact is that the amount of e-donor is able to reduce whole amount of e-acceptor of the system.
369 This explains the fact that the temporal evolutions of NO₂⁻ and N₂O (Fig. 4-C and Fig. 4-D) in the anaerobic conditions
370 hit zero, increasing the value of the GRI.

371 The simulated data for the drymass evolution in experiment E1 and E2 has the lowest GRI values. These results reinforce
372 the idea that the contribution of TEEM2 to write the metabolic reactions is crucial in a model based on individuals and
373 moreover that the metabolism is a central part of it. Also, it suggests that the formula C₃H_{5.4}O_{1.45}N_{0.75} used to represent
374 the biomass of *P. denitrificans* provides an acceptable agreement between the simulated and experimental system
375 variables.

376 The system variables outputs for *P. denitrificans* with INDISIM-Denitrification simulator improve the GRI value, from
377 12.94 (INDISIM-Paracoccus) to 2.02 (INDISIM-Denitrification), for the N₂O time evolution for the experiment with e-
378 donor limited (Fig. 3-D) in relation to the results presented in our previous work [31]. In light of this results it seems
379 plausible that the individual-mass degradation could be an interesting individual strategy to reduce the accumulation of
380 cytotoxic products in the surrounding media as has been pointed out by some authors [22].

381 In addition to those temporal evolutions which are compared to the experimental values through GRI values, INDISIM-
382 Denitrification gives the outputs (graphical and numerical) for other nutrients and metabolic products involved in the
383 denitrification process, such as succinate, NH₄⁺, O₂, NO, N₂, CO₂ and HCO₃⁻ (Fig. 2). These chemical compounds do not
384 have the corresponding experimental temporal evolutions in the data set presented by Felgate et al. (2012), therefore it is
385 not possible to calculate the GRI values for them. However, INDISIM-Denitrification provides the user with these data
386 and thus, it makes possible a comparison when new experimental data become available.

387 **3.3.2 Simulations for *A. xylooxidans***

388 We took new experimental data published by Felgate et al. (2012), and not previously used, into account for comparing
389 the adequacy of the simulations with INDISIM-Denitrification for *A. xylooxidans*, to evaluate the goodness of the model,
390 and to assess the improvements introduced to achieve the objectives of this work. Simulations were run with the empirical
391 chemical formula C₅H₉O_{2.5}N, which is commonly used to represent the biomass composition of *A. xylooxidans*. The

392 individual and environmental parameter values that caused model outputs with acceptable GRI coefficient are shown in
393 Table 12.

394 In Figure 5 and Figure 6, the outputs assessed for the bacterium *A. xylosoxidans* are shown, namely the drymass, NO_3^- ,
395 NO_2^- and N_2O evolutions for the two experiments, experiment E1 with succinate-limited/ NO_3^- -sufficient (Fig. 5) and
396 experiment E2 with succinate-sufficient/ NO_3^- -limited (Fig. 6), where the GRI scores obtained in the statistical analysis
397 performed are included. According to the GRI values for the experiment e-donor limited (Fig. 5), the simulation results
398 obtained with INDISIM-Denitrification for the bacterium *A. xylosoxidans* showed an acceptable behavior, because all of
399 the values were in the acceptable range of GRI (from 1 to 3). The highest GRI value was obtained in the temporal evolution
400 of NO_2^- (Fig. 5-C).

401 The acceptable range for GRI was only achieved in the drymass and NO_3^- evolution (Fig. 6-A and Fig. 6-B) for the
402 experiment e-donor sufficient (E2). This model's behavior is a key point for future upgrades of this INDISIM branch
403 because it could be necessary to include a new behavior-rule at the individual level to regulate the model's response when
404 the e-acceptor is limited (e-donor sufficient).

405 **4. Conclusions and final remarks**

406 Considering the GRI values obtained for the temporal evolutions variables tested, INDISIM-Denitrification provides
407 acceptable results for the experiments where the e-donor is limited, specifically for denitrifying bacterium *P. denitrificans*:
408 (a) biomass, from 1.22 (INDISIM-Paracoccus) to 1.08 (INDISIM-Denitrification), (b) nitrate, from 1.26 (INDISIM-
409 Paracoccus) to 1.23 (INDISIM-Denitrification), (c) nitrite, from 2.05 (INDISIM-Paracoccus) to 1.97 (INDISIM-
410 Denitrification), and (d) nitrous oxide, from 12.94 (INDISIM-Paracoccus) to 2.02 (INDISIM-Denitrification) (Fig. 3 and
411 Fig. 5). We consider that one of the reasons is due to TEEM being designed for bacterial yield prediction in microbial
412 systems when the C-source is a limiting factor, e.g. the wastewater treatments [22].

413 One of the novelties of INDISIM-Denitrification simulator is that it offers a greater versatility in relation to the previous
414 version (INDISIM-Paracoccus), because it can be used to work with any other bacteria in a pure culture. It is also possible
415 to simulate a functional denitrifying group when the user works with mixed cultures and use mean molar coefficient for
416 microbial biomass (n,a,b,c) defining a representative empirical formula for bacterial population. In consequence, all the
417 stoichiometric coefficients for the set of MMRs for each metabolic pathway are automatically recalculated. Following
418 the principle that all individuals could achieve the maximum growth rate, μ_{\max} if the user changes this value, the individual
419 maximum uptake-rate values are recalculated for all nutrients involved in metabolism, according to the stoichiometric
420 coefficients of the MMRs related with individual mass synthesis. Since these improvements in the parameter calculations
421 are incorporated in the code, the calibration for other denitrifying populations is easier. Therefore, the INDISIM-

422 Denitrification simulator allows the user to interact in a much more extensive way with significant biological parameters
423 of the metabolic part of the bacteria, giving different values to parameters that can condition the growth dynamics, and
424 which are notable for the denitrification results.

425 The model has been improved since we have assumed that individuals cannot live and develop in the same way in a
426 favorable environment as in a hostile environment. From the moment in which an accumulation of cytotoxic products
427 occurs in the medium, the individual develops a strategy to survive and it has an energy or mass cost. We have assumed
428 that the individual consumes its own biomass to reduce some of the N-oxides which are toxic and we have implemented
429 this sub model as a part of the metabolism. This assumption has given much better results in the calibration of the model
430 in relation to the INDISIM-Paracoccus, specifically for the evolution of NO and N₂O for both bacteria in the experiment
431 succinate-limited/NO₃⁻-sufficient, since accumulation did not occur in the simulated system just as in the experimental
432 tests. So, we can conclude that our assumption or hypothesis is consistent and reflects how individuals maintain their
433 viability in the presence of cytotoxic products.

434 The implementation of INDISIM-Denitrification in NetLogo offers easy access to the computer code for future and
435 specific adaptations to the user interested in diverse academic and research applications. In particular, it facilitates the
436 exploration of the effects of bacterial metabolic behavior on denitrification dynamics and allows users to test their own
437 (virtual or measured) parameter values or to compare the model output to their own observations.

438 Based on results, it appears that INDISIM-Denitrification is a useful tool to model any denitrifying bacterium in batch
439 and continuous cultures under different oxygen concentration to simulate aerobic or anaerobic metabolism. In this study,
440 homogeneous, laboratory chemostat data, typically showing low spatial heterogeneity, have been used. Nevertheless, the
441 developed model allows us to include the heterogeneous dynamics into the system. This heterogeneity is not only related
442 with aerobic and anaerobic conditions, it is also reflected at the individual level with the behavior rules and alternatives
443 in the use of metabolic pathways. For instance, the heterogeneity at individual level can be revealed using biomass
444 distributions of the bacteria (or other distributions of cellular contents) and controlling which reactions are more often
445 used than others by the microbes during the temporal evolution of the system (Figure 2). Nowadays, this perspective on
446 the biological heterogeneity in individual behavior has been assumed and treated in other applications [100–102] in order
447 to advance our understanding of microbial systems. Using highly controlled experimental conditions has offered the
448 possibility to focus on the individual behavior rules (exception made of the bacterial movement) that are now validated
449 and ready, in the near future, to deal with other medium conditions.

450 TEEM2, one of the thermodynamic models based on bioenergetics growth efficiency, also appears to be a useful tool for
451 modeling the individual metabolism in the INDISIM-Denitrification model. In contrast to other modeling approaches, it
452 allows the user to embed thermodynamic properties into individual cells, which can simulate the behavior of the bacterial

453 population more realistically than the continuous and traditional population-based approaches.

454 With μ IBM as the INDISIM-Denitrification it should be possible to investigate the theory for the coupling energy between
455 catabolism and the anabolism, which is the principal assumption in the TEEM2 because it considers that thermodynamic
456 free energy is lost at each transfer by including a term for this efficiency (ε). TEEM2 considers ε value constant, but there
457 is no clear reason why it should do this. Therefore, experiments could be developed with some specific environmental
458 conditions where the same metabolic pathway would be adjusted with different values of ε . The use of IBMs allow to
459 model individuals that can change their (ε) value according to the local environmental conditions. This will be an
460 interesting contribution because some authors consider that ε value is not constant in the metabolic process [76, 77].

461 The development and application of μ IBM with some intracellular detail and complexity is the key advantage of our new
462 model for studying the different steps of denitrification carried out by a denitrifying bacterium. Exploring model behavior
463 via its input parameters and assessing alternative sub-models provides a way to progress with the development of a
464 simulator able to control factors that contribute to our understanding of how major or minor N_2O generation is a
465 consequence of this denitrified metabolic individual activity.

466 In a broader context, and in connection with other models where the process of nitrification can be significant, this model
467 can give insights into the representation of microbial activity existing in diverse environments, as for instance, in organic
468 matter transformations. For instance, the mineralization and nitrification processes involved in those transformations are
469 mainly driven by bacteria (and other microbes), and consequently, the standpoint used in this denitrifying model can be
470 adapted or incorporated to represent these processes [68, 69]. The cycles of carbon and nitrogen require the integration
471 of these interacting processes. The challenges associated with the distribution and activity of microorganisms at a
472 microscale, for instance, in soils, is being investigated both from experimental data with advanced and innovative
473 techniques and with the use of models and simulations [103]. Insights of the microscale heterogeneity of the spatial
474 distribution of organic matter connected with microbial activity need spatially explicit modelling approaches. In the recent
475 past computer simulations focusing on the microscale are resulting in some additions to our understanding of such
476 complex environments [104–106]. The denitrifying model achieved in this study would highly benefit those spatially
477 explicit models, because it can be treated as a module in order to build the backbone of a more ambitious biophysical
478 model for transformations of organic matter.

479 **Acknowledgments**

480 The financial support of the Ecuador National Secretary of Higher Education, Science, Technology and Innovation
481 (SENESCYT) (Grant *Convocatoria Abierta 2011* – no. 94-2012), to the Universidad Central del Ecuador (Research
482 Project no. 26 according to RHCU.SO.08 No. 0082-2017 in official resolution with date March 21th, 2017) and the Plan

483 Nacional I+D+i from the Spanish Ministerio de Educación y Ciencia (MICINN, CGL2010-20160). We would also like
484 to thank Dr. David Richardson and Dr. Andrew Gates for helpful discussions at early stages in this project and for
485 providing us with the full dataset presented in Felgate et al. (2012).

486 **Authors Contributions**

487 All authors listed, have made substantial, direct and intellectual contribution to the work, and approved it for publication.

488 **Conflict of Interest Statement**

489 The authors declare that the research was conducted in the absence of any commercial or financial relationships that could
490 be construed as a potential conflict of interest.

491

- 493 1. Zumft W (1997) Cell biology and molecular basis of denitrification. *Microbiol Mol Biol Rev* 61:533–616
- 494 2. Baumann B, Snozzi M, Zehnder A, Van Der Meer J (1996) Dynamics of denitrification activity of *Paracoccus*
495 *denitrificans* in continuous culture during aerobic-anaerobic changes. *J Bacteriol* 178:4367–4374
- 496 3. Blackburn TH (1990) *Denitrification in Soil and Sediment*. Springer US, Boston, MA
- 497 4. Ye RW, Averill BA, Tiedje JM (1994) Denitrification: production and consumption of nitric oxide. *Appl Environ*
498 *Microbiol* 60:1053–8
- 499 5. Bergaust L, van Spanning RJM, Frostegård A, Bakken LR (2012) Expression of nitrous oxide reductase in
500 *Paracoccus denitrificans* is regulated by oxygen and nitric oxide through FnrP and NNR. *Microbiology* 158:826–
501 34. <https://doi.org/10.1099/mic.0.054148-0>
- 502 6. Berks BC, Ferguson SJ, Moir JWB, Richardson DJ (1995) Enzymes and associated electron transport systems
503 that catalyse the respiratory reduction of nitrogen oxides and oxyanions. *Biochim Biophys Acta - Bioenerg*
504 1232:97–173. [https://doi.org/10.1016/0005-2728\(95\)00092-5](https://doi.org/10.1016/0005-2728(95)00092-5)
- 505 7. Drummond JT, Matthews RG (1994) Nitrous Oxide Degradation by Cobalamin-Dependent Methionine Synthase:
506 Characterization of the Reactants and Products in the Inactivation Reaction. *Biochemistry* 33:3732–3741.
507 <https://doi.org/10.1021/bi00178a033>
- 508 8. Hochstein LI, Tomlinson GA (1988) The enzymes associated with denitrification. *Annu Rev Microbiol* 42:231–
509 61. <https://doi.org/10.1146/annurev.mi.42.100188.001311>
- 510 9. Snyder SW, Hollocher TC (1987) Purification and some characteristics of nitrous oxide reductase from
511 *Paracoccus denitrificans*. *J Biol Chem* 262:6515–6525
- 512 10. Zumft WG, Körner H (1997) Enzyme diversity and mosaic gene organization in denitrification. *Antonie Van*
513 *Leeuwenhoek* 71:43–58. <https://doi.org/10.1023/A:1000112008026>
- 514 11. Bergaust L, Mao Y, Bakken LR, Frostegård A (2010) Denitrification response patterns during the transition to
515 anoxic respiration and posttranscriptional effects of suboptimal pH on nitrous [corrected] oxide reductase in
516 *Paracoccus denitrificans*. *Appl Environ Microbiol* 76:6387–96. <https://doi.org/10.1128/AEM.00608-10>
- 517 12. Caspi R, Altman T, Dreher K, et al (2012) The MetaCyc database of metabolic pathways and enzymes and the
518 BioCyc collection of pathway/genome databases. *Nucleic Acids Res* 40:D742-53.
519 <https://doi.org/10.1093/nar/gkr1014>
- 520 13. Hernandez D, Rowe JJ (1987) Oxygen regulation of nitrate uptake in denitrifying *Pseudomonas aeruginosa*. *Appl*
521 *Environ Microbiol* 53:745–50
- 522 14. Stouthamer AH (1991) Metabolic regulation including anaerobic metabolism in *Paracoccus denitrificans*. *J*
523 *Bioenerg Biomembr* 23:163–185
- 524 15. Davidson EA, Kingerlee W (1997) A global inventory of nitric oxide emissions from soils. *Nutr Cycl*
525 *Agroecosystems* 48:37–50. <https://doi.org/10.1023/A:1009738715891>
- 526 16. Farquharson R, Baldock J (2007) Concepts in modelling N₂O emissions from land use. *Plant Soil* 309:147–167.
527 <https://doi.org/10.1007/s11104-007-9485-0>
- 528 17. Smith KA, Clayton H, McTaggart IP, et al (1995) The Measurement of Nitrous Oxide Emissions from Soil by
529 Using Chambers [and Discussion]. *Philos Trans R Soc A Math Phys Eng Sci* 351:327–338.
530 <https://doi.org/10.1098/rsta.1995.0037>
- 531 18. Felgate H, Giannopoulos G, Sullivan MJ, et al (2012) The impact of copper, nitrate and carbon status on the
532 emission of nitrous oxide by two species of bacteria with biochemically distinct denitrification pathways. *Environ*
533 *Microbiol* 14:1788–800. <https://doi.org/10.1111/j.1462-2920.2012.02789.x>
- 534 19. Richardson D, Felgate H, Watmough N, et al (2009) Mitigating release of the potent greenhouse gas N(2)O from
535 the nitrogen cycle - could enzymic regulation hold the key? *Trends Biotechnol* 27:388–97.
536 <https://doi.org/10.1016/j.tibtech.2009.03.009>
- 537 20. Sullivan MJ, Gates AJ, Appia-Ayme C, et al (2013) Copper control of bacterial nitrous oxide emission and its
538 impact on vitamin B12-dependent metabolism. *Proc Natl Acad Sci U S A* 110:19926–31.
539 <https://doi.org/10.1073/pnas.1314529110>

- 540 21. Henze M, Gujer W, Mino T, van Loosedrecht M (2006) Activated Sludge Models ASM1, ASM2, ASM2d and
541 ASM3
- 542 22. Rittmann BE, McCarty PL (2001) Environmental Biotechnology: Principles and Applications
- 543 23. Davidson EA, Keller M, Erickson HE, et al (2000) Testing a Conceptual Model of Soil Emissions of Nitrous and
544 Nitric Oxides. *Bioscience* 50:667. [https://doi.org/10.1641/0006-3568\(2000\)050\[0667:TACMOS\]2.0.CO;2](https://doi.org/10.1641/0006-3568(2000)050[0667:TACMOS]2.0.CO;2)
- 545 24. Heinen M (2006) Simplified denitrification models: Overview and properties. *Geoderma* 133:444–463.
546 <https://doi.org/10.1016/j.geoderma.2005.06.010>
- 547 25. Hu Z, Chandran K, Grasso D, Smets BF (2004) Comparison of nitrification inhibition by metals in batch and
548 continuous flow reactors. *Water Res* 38:3949–59. <https://doi.org/10.1016/j.watres.2004.06.025>
- 549 26. Kampschreur MJ, Kleerebezem R, Picioreanu C, et al (2012) Metabolic modeling of denitrification in
550 *Agrobacterium tumefaciens*: a tool to study inhibiting and activating compounds for the denitrification pathway.
551 *Front Microbiol* 3:370. <https://doi.org/10.3389/fmicb.2012.00370>
- 552 27. Parton WJ, Mosier AR, Ojima DS, et al (1996) Generalized model for N₂ and N₂O production from nitrification
553 and denitrification. *Global Biogeochem Cycles* 10:401–412. <https://doi.org/10.1029/96GB01455>
- 554 28. Woolfenden HC, Gates AJ, Bocking C, et al (2013) Modeling the effect of copper availability on bacterial
555 denitrification. *Microbiologyopen* 2:756–65. <https://doi.org/10.1002/mbo3.111>
- 556 29. Araujo Granda P, Gras A, Ginovart M (2014) An Individual-based model for the study of *Paracoccus*
557 *denitrificans*, a denitrifying bacterium. In: Méndez-Vilas A (ed) Industrial, medical and environmental
558 applications of microorganisms. Current status and trends. Wageningen Academic Publishers, pp 28–33
- 559 30. Araujo Granda P, Gras A, Ginovart M (2015) Thermodynamic behavior-rules for a bacterial individual-based
560 model to study the denitrification process. *IFAC-PapersOnLine* 48:743–748.
561 <https://doi.org/10.1016/j.ifacol.2015.05.015>
- 562 31. Araujo Granda P, Gras A, Ginovart M, Moulton V (2016) INDISIM-*Paracoccus*, an individual-based and
563 thermodynamic model for a denitrifying bacterium. *J Theor Biol* 403:45–58.
564 <https://doi.org/10.1016/j.jtbi.2016.05.017>
- 565 32. Araujo Granda P, Gras A, Ginovart M (2016) Mass degradation to reduce cytotoxic products as an individual
566 behavior-rule embedded in a microbial model for the study of the denitrification process. In: A. Méndez-Vilas
567 (ed) *Microbes in the spotlight: recent progress in the understanding of beneficial and harmful microorganisms*.
568 BrownWalker Press, pp 444-448 (both included)
- 569 33. Lu H, Chandran K, Stensel D (2014) Microbial ecology of denitrification in biological wastewater treatment.
570 *Water Res*. <https://doi.org/10.1016/j.watres.2014.06.042>
- 571 34. Snyder CS, Bruulsema TW, Jensen TL, Fixen PE (2009) Review of greenhouse gas emissions from crop
572 production systems and fertilizer management effects. *Agric Ecosyst Environ* 133:247–266.
573 <https://doi.org/10.1016/j.agee.2009.04.021>
- 574 35. Davidson EA, Rogers J., Whitman WB (1991) Fluxes of nitrous oxide and nitric oxide from terrestrial
575 ecosystems. 219–235
- 576 36. Knowles R (1982) Denitrification. *Microbiol Rev* 46:43–70
- 577 37. Holt J, Krieg N, Sneath P, et al (1994) International edition: Bergey's manual of determinative bacteriology
- 578 38. Drummond JT, Matthews RG (1994) Nitrous Oxide Inactivation of Cobalamin-Dependent Methionine Synthase
579 from *Escherichia coli*: Characterization of the Damage to the Enzyme and Prosthetic Group. *Biochemistry*
580 33:3742–3750. <https://doi.org/10.1021/bi00178a034>
- 581 39. Shuler ML, Kargi F (2002) Bioprocess engineering : basic concepts. Prentice Hall
- 582 40. Railsback SF, Grimm V (2012) Agent-Based and Individual-Based Modeling: A Practical Introduction. Princeton
583 University Press
- 584 41. Cardona M, Colomer MA, Margalida A, et al (2010) A P System Based Model of an Ecosystem of Some
585 Scavenger Birds. In: *Membrane Computing*. Springer Berlin Heidelberg, pp 182–195
- 586 42. Ferrer J, Prats C, López D (2008) Individual-based modelling: an essential tool for microbiology. *J Biol Phys*
587 34:19–37. <https://doi.org/10.1007/s10867-008-9082-3>
- 588 43. Garcia-Ochoa F, Gomez E, Santos VE, Merchuk JC (2010) Oxygen uptake rate in microbial processes: An
589 overview. *Biochem Eng J* 49:289–307. <https://doi.org/10.1016/j.bej.2010.01.011>

- 590 44. Raaijmakers JM, Vlami M, de Souza JT (2002) Antibiotic production by bacterial biocontrol agents. *Antonie Van*
591 *Leeuwenhoek* 81:537–547. <https://doi.org/10.1023/A:1020501420831>
- 592 45. Resat H, Bailey V, McCue LA, Konopka A (2012) Modeling microbial dynamics in heterogeneous environments:
593 growth on soil carbon sources. *Microb Ecol* 63:883–97. <https://doi.org/10.1007/s00248-011-9965-x>
- 594 46. Araujo Granda P (2017) Developing an individual-based model to study the bacterial denitrification process
595 (Ph.D. Thesis). Universitat Politècnica de Catalunya
596 <http://repositorio.educacionsuperior.gob.ec/handle/28000/4244>
- 597 47. Grimm V (1999) Ten years of individual-based modelling in ecology: what have we learned and what could we
598 learn in the future? *Ecol Modell* 115:129–148. [https://doi.org/10.1016/S0304-3800\(98\)00188-4](https://doi.org/10.1016/S0304-3800(98)00188-4)
- 599 48. Grimm V, Berger U, Bastiansen F, et al (2006) A standard protocol for describing individual-based and agent-
600 based models. *Ecol Modell* 198:115–126. <https://doi.org/10.1016/j.ecolmodel.2006.04.023>
- 601 49. Kreft J-U, Plugge CM, Grimm V, et al (2013) Mighty small: Observing and modeling individual microbes
602 becomes big science. *Proc Natl Acad Sci U S A* 110:18027–8. <https://doi.org/10.1073/pnas.1317472110>
- 603 50. Railsback SF, Johnson MD (2011) Pattern-oriented modeling of bird foraging and pest control in coffee farms.
604 *Ecol Modell* 222:3305–3319. <https://doi.org/10.1016/j.ecolmodel.2011.07.009>
- 605 51. Reuter H, Breckling B, Jopp F (2011) Individual-Based Models. In: Jopp F, Reuter H, Breckling B (eds)
606 *Modelling Complex Ecological Dynamics*. Springer Berlin Heidelberg, Berlin, Heidelberg, pp 163–178
- 607 52. Hellweger FL, Bucci V (2009) A bunch of tiny individuals—Individual-based modeling for microbes. *Ecol*
608 *Modell* 220:8–22. <https://doi.org/10.1016/j.ecolmodel.2008.09.004>
- 609 53. Portell X, Gras A, Ginovart M (2014) INDISIM-Saccha, an individual-based model to tackle *Saccharomyces*
610 *cerevisiae* fermentations. *Ecol Modell* 279:12–23. <https://doi.org/10.1016/j.ecolmodel.2014.02.007>
- 611 54. Tack ILMM, Logist F, Noriega Fernandez E, Van Impe JFM (2015) An individual-based modeling approach to
612 simulate the effects of cellular nutrient competition on *Escherichia coli* K-12 MG1655 colony behavior and
613 interactions in aerobic structured food systems. *Food Microbiol* 45:179–188.
614 <https://doi.org/10.1016/j.fm.2014.05.003>
- 615 55. Hellweger FL, Clegg RJ, Clark JR, et al (2016) Advancing microbial sciences by individual-based modelling.
616 *Nat Rev Microbiol* 14:461–471. <https://doi.org/10.1038/nrmicro.2016.62>
- 617 56. Thiele JC, Grimm V (2010) NetLogo meets R: Linking agent-based models with a toolbox for their analysis.
618 *Environ Model Softw* 25:972–974. <https://doi.org/10.1016/j.envsoft.2010.02.008>
- 619 57. Wilensky U (1999) NetLogo. In: *Cent. Connect. Learn. Comput. Model. Northwest. Univ. Evanston, IL.*
620 <http://ccl.northwestern.edu/netlogo/>. Accessed 5 Mar 2014
- 621 58. Ginovart M (2014) Discovering the Power of Individual-Based Modelling in Teaching and Learning: The Study
622 of a Predator-Prey System. *J Sci Educ Technol* 23:1–18. <https://doi.org/10.1007/s10956-013-9480-6>
- 623 59. Ginovart M, Prats C (2012) A Bacterial Individual-Based Virtual Bioreactor to Test Handling Protocols in a
624 Netlogo Platform. In: *Mathematical Modelling*. pp 647–652
- 625 60. Ginovart M, Portell X, Ferrer-Closas P (2012) Modelización Basada En El Individuo: Una Metodología
626 Atractiva. *Enseñanza Las Ciencias* 30:93–108
- 627 61. Font-Marques M, Ginovart M (2016) Modelización de crecimientos microbianos en medios heterogéneos y de
628 movilidad reducida. *Model Sci Educ Learn* 9:81–120. <https://doi.org/10.4995/MSEL.2016.5789>
- 629 62. Thiele JC, Kurth W, Grimm V (2012) RNETLOGO: an R package for running and exploring individual-based
630 models implemented in NETLOGO. *Methods Ecol Evol* 3:480–483. <https://doi.org/10.1111/j.2041-210X.2011.00180.x>
- 631
- 632 63. Thiele JC, Kurth W, Grimm V (2012) Agent-Based Modelling: Tools for Linking NetLogo and R
- 633 64. Thiele JC (2014) R marries NetLogo: introduction to the RNetLogo package. *J Stat*
- 634 65. Thiele JC, Kurth W, Grimm V (2014) Facilitating Parameter Estimation and Sensitivity Analysis of Agent-Based
635 Models: A Cookbook Using NetLogo and “R.” *J Artif Soc Soc Simul* 17:11
- 636 66. Ginovart M, López D, Valls J (2002) INDISIM, an individual-based discrete simulation model to study bacterial
637 cultures. *J Theor Biol* 214:305–19. <https://doi.org/10.1006/jtbi.2001.2466>

- 638 67. Ginovart M, López D, Gras A (2005) Individual-based modelling of microbial activity to study mineralization of
639 C and N and nitrification process in soil. *Nonlinear Anal Real World Appl* 6:773–795.
640 <https://doi.org/10.1016/j.nonrwa.2004.12.005>
- 641 68. Gras A, Ginovart M, Valls J, Baveye PC (2011) Individual-based modelling of carbon and nitrogen dynamics in
642 soils: Parameterization and sensitivity analysis of microbial components. *Ecol Modell* 222:1998–2010.
643 <https://doi.org/10.1016/j.ecolmodel.2011.03.009>
- 644 69. Banitz T, Gras A, Ginovart M (2015) Individual-based modeling of soil organic matter in NetLogo: Transparent,
645 user-friendly, and open. *Environ Model Softw* 71:39–45. <https://doi.org/10.1016/j.envsoft.2015.05.007>
- 646 70. Ginovart M, Cañadas JC (2008) INDISIM-YEAST: an individual-based simulator on a website for experimenting
647 and investigating diverse dynamics of yeast populations in liquid media. *J Ind Microbiol Biotechnol* 35:1359–66.
648 <https://doi.org/10.1007/s10295-008-0436-4>
- 649 71. Prats C, Ferrer J, Gras A, Ginovart M (2010) Individual-based modelling and simulation of microbial processes:
650 yeast fermentation and multi-species composting. *Math Comput Model Dyn Syst* 16:489–510.
651 <https://doi.org/10.1080/13873954.2010.481809>
- 652 72. Cogne G, Rügen M, Bockmayr A, et al (2011) A model-based method for investigating bioenergetic processes in
653 autotrophically growing eukaryotic microalgae: application to the green algae *Chlamydomonas reinhardtii*.
654 *Biotechnol Prog* 27:631–40. <https://doi.org/10.1002/btpr.596>
- 655 73. Toussaint O, Schneider ED (1998) The thermodynamics and evolution of complexity in biological systems. *Comp*
656 *Biochem Physiol - A Mol Integr Physiol* 120:3–9. [https://doi.org/10.1016/S1095-6433\(98\)10002-8](https://doi.org/10.1016/S1095-6433(98)10002-8)
- 657 74. McCarty PL (2007) Thermodynamic electron equivalents model for bacterial yield prediction: modifications and
658 comparative evaluations. *Biotechnol Bioeng* 97:377–388. <https://doi.org/10.1002/bit>
- 659 75. von Stockar U, van der Wielen LAM (1997) Thermodynamics in biochemical engineering. *J Biotechnol* 59:25–
660 37. [https://doi.org/10.1016/S0168-1656\(97\)00167-3](https://doi.org/10.1016/S0168-1656(97)00167-3)
- 661 76. Xiao J, VanBriesen JM (2006) Expanded thermodynamic model for microbial true yield prediction. *Biotechnol*
662 *Bioeng* 93:110–21. <https://doi.org/10.1002/bit.20700>
- 663 77. Xiao J, VanBriesen JM (2008) Expanded thermodynamic true yield prediction model: adjustments and
664 limitations. *Biodegradation* 19:99–127. <https://doi.org/10.1007/s10532-007-9119-5>
- 665 78. Demirel Y (2010) Nonequilibrium thermodynamics modeling of coupled biochemical cycles in living cells. *J*
666 *Nonnewton Fluid Mech* 165:953–972. <https://doi.org/10.1016/j.jnnfm.2010.02.006>
- 667 79. Roels JA (1980) Application of macroscopic principles to microbial metabolism. *Biotechnol Bioeng* 103:2–59;
668 discussion 1. <https://doi.org/10.1002/bit.260221202>
- 669 80. Roels JA (1983) *Energetics and kinetics in biotechnology*. Elsevier Biomedical Press, Amsterdam
- 670 81. Christensen D, McCarty PL (1975) Multi-process biological treatment model. *J (Water Pollut Control Fed*
671 *47:2652–2664*
- 672 82. Heijnen JJ, van Loosdrecht MCM, Tijhuis L (1992) A Black Box Mathematical Model to Calculate Auto- and
673 Heterotrophic Biomass Yields based on Gibbs Energy Dissipation. *Biotechnol Bioeng* 40:1139–1154
- 674 83. Heijnen JJ (1999) Bioenergetics of microbial growth. *Encycl. Bioprocess Technol. Ferment. Biocatal. Biosep.*
675 *267–291*
- 676 84. Heijnen JJ, Van Dijken JP (1992) In search of a thermodynamic description of biomass yields for the
677 chemotrophic growth of microorganisms. *Biotechnol Bioeng* 39:833–58. <https://doi.org/10.1002/bit.260390806>
- 678 85. Tijhuis L, Van Loosdrecht MC, Heijnen JJ (1993) A thermodynamically based correlation for maintenance gibbs
679 energy requirements in aerobic and anaerobic chemotrophic growth. *Biotechnol Bioeng* 42:509–519.
680 <https://doi.org/10.1002/bit.260420415>
- 681 86. Liu J-S, Vojinović V, Patiño R, et al (2007) A comparison of various Gibbs energy dissipation correlations for
682 predicting microbial growth yields. *Thermochim Acta* 458:38–46. <https://doi.org/10.1016/j.tca.2007.01.016>
- 683 87. von Stockar U, Maskow T, Liu J, et al (2006) Thermodynamics of microbial growth and metabolism: an analysis
684 of the current situation. *J Biotechnol* 121:517–33. <https://doi.org/10.1016/j.jbiotec.2005.08.012>
- 685 88. McCarty PL (1971) Energetics and bacterial growth. *Org Compd Aquat Environ* 1:157–172
- 686 89. Stratton FE, McCarty PL (1969) Graphical evaluation of the kinetic parameters for bacterial growth. *Can J*
687 *Microbiol* 15:1201–1205. <https://doi.org/10.1139/m69-217>

- 688 90. McCarty P (1965) Thermodynamics of biological synthesis and growth. *Int J Air Water Pollut* 621–639
- 689 91. VanBriesen JM, Rittmann BE (2000) Mathematical description of microbiological reactions involving
690 intermediates. *Biotechnol Bioeng* 67:35–52
- 691 92. VanBriesen JM (2002) Evaluation of methods to predict bacterial yield using thermodynamics. *Biodegradation*
692 13:171–190. <https://doi.org/10.1023/A:1020887214879>
- 693 93. Jachner S, van den Boogaart KG, Petzoldt T (2007) Statistical Methods for the Qualitative Assessment of
694 Dynamic Models with Time Delay (R Package qualV). *J Stat Softw* 22:1–30
- 695 94. Leggett RW, Williams LR (1981) A reliability index for models. *Ecol Modell* 13:303–312.
696 [https://doi.org/10.1016/0304-3800\(81\)90034-X](https://doi.org/10.1016/0304-3800(81)90034-X)
- 697 95. Grimm V, Berger U, DeAngelis DL, et al (2010) The ODD protocol: A review and first update. *Ecol Modell*
698 221:2760–2768. <https://doi.org/10.1016/j.ecolmodel.2010.08.019>
- 699 96. van Verseveld HW, Braster M, Boogerd FC, et al (1983) Energetic aspects of growth of *Paracoccus denitrificans*:
700 oxygen-limitation and shift from anaerobic nitrate-limitation to aerobic succinate-limitation. *Arch Microbiol*
701 135:229–236. <https://doi.org/10.1007/BF00414485>
- 702 97. van Verseveld HW, Boon JP, Stouthamer AH (1979) Growth yields and the efficiency of oxidative
703 phosphorylation of *Paracoccus denitrificans* during two- (carbon) substrate-limited growth. *Arch Microbiol*
704 121:213–223. <https://doi.org/10.1007/BF00425058>
- 705 98. van Verseveld HW, Meijer EM, Stouthamer AH (1977) Energy conservation during nitrate respiration in
706 *Paracoccus denitrificans*. *Arch Microbiol* 112:17–23. <https://doi.org/10.1007/BF00446649>
- 707 99. Nielsen DR, McLellan PJ, Daugulis AJ (2006) Direct estimation of the oxygen requirements of *Achromobacter*
708 *xylooxidans* for aerobic degradation of monoaromatic hydrocarbons (BTEX) in a bioscrubber. *Biotechnol Lett*
709 28:1293–8. <https://doi.org/10.1007/s10529-006-9093-8>
- 710 100. González-Cabaleiro R, Mitchell AM, Smith W, et al (2017) Heterogeneity in Pure Microbial Systems:
711 Experimental Measurements and Modeling. *Front Microbiol* 8:1813. <https://doi.org/10.3389/fmicb.2017.01813>
- 712 101. Kreft J-U, Plugge CM, Prats C, et al (2017) From Genes to Ecosystems in Microbiology: Modeling Approaches
713 and the Importance of Individuality. *Front Microbiol* 8:2299. <https://doi.org/10.3389/fmicb.2017.02299>
- 714 102. Gogulancea V, González-Cabaleiro R, Li B, et al (2019) Individual Based Model Links Thermodynamics,
715 Chemical Speciation and Environmental Conditions to Microbial Growth. *Front Microbiol* 10:1871.
716 <https://doi.org/10.3389/fmicb.2019.01871>
- 717 103. Baveye PC, Otten W, Kravchenko A (2019) Editorial: Elucidating Microbial Processes in Soils and Sediments:
718 Microscale Measurements and Modeling. *Front Environ Sci* 7:78. <https://doi.org/10.3389/fenvs.2019.00078>
- 719 104. Falconer RE, Battaia G, Schmidt S, et al (2015) Microscale Heterogeneity Explains Experimental Variability and
720 Non-Linearity in Soil Organic Matter Mineralisation. *PLoS One* 10:e0123774.
721 <https://doi.org/10.1371/journal.pone.0123774>
- 722 105. Cooper LJ, Daly KR, Hallett PD, et al (2018) The effect of root exudates on rhizosphere water dynamics. *Proc R*
723 *Soc A Math Phys Eng Sci* 474:20180149. <https://doi.org/10.1098/rspa.2018.0149>
- 724 106. Portell X, Pot V, Garnier P, et al (2018) Microscale Heterogeneity of the Spatial Distribution of Organic Matter
725 Can Promote Bacterial Biodiversity in Soils: Insights From Computer Simulations. *Front Microbiol* 9:1583.
726 <https://doi.org/10.3389/fmicb.2018.01583>

727

728

Table 1. Microbial metabolic reactions (Energy Reactions - Re) for cellular maintenance in aerobic (I) and anaerobic phase (from II to V). Re = Ra - Rd according to TEEM2 [22, 74].

I	$(\text{C}_4\text{H}_4\text{O}_4)^{2-} + 3.5 \text{O}_2 = 2 \text{CO}_2 + 2 \text{HCO}_3^- + \text{H}_2\text{O}$
II	$(\text{C}_4\text{H}_4\text{O}_4)^{2-} + 7 \text{NO}_3^- = 7 \text{NO}_2^- + 2 \text{CO}_2 + 2 \text{HCO}_3^- + \text{H}_2\text{O}$
III	$(\text{C}_4\text{H}_4\text{O}_4)^{2-} + 14 \text{NO}_2^- + 14 \text{H}^+ = 14 \text{NO} + 2 \text{CO}_2 + 2 \text{HCO}_3^- + 8 \text{H}_2\text{O}$
IV	$(\text{C}_4\text{H}_4\text{O}_4)^{2-} + 14 \text{NO} = 7 \text{N}_2\text{O} + 2 \text{CO}_2 + 2 \text{HCO}_3^- + \text{H}_2\text{O}$
V	$(\text{C}_4\text{H}_4\text{O}_4)^{2-} + 7 \text{N}_2\text{O} = 7 \text{N}_2 + 2 \text{CO}_2 + 2 \text{HCO}_3^- + \text{H}_2\text{O}$

729

Table 2. Microbial metabolic reactions for individual-mass synthesis in aerobic^(a) and anaerobic^(b) conditions for any denitrifying bacteria when succinate is C-source, NH₄⁺ is N-source and different e-acceptors involved in common denitrification pathway. (R = fe^o Ra + fs^o Rc - Rd) according to TEEM2 [22, 74].

I(a)	$\left(\frac{1}{14}\right) C_4H_4O_4^{2-} + \left(f_s^o \frac{c}{d}\right) NH_4^+ + \left(\frac{1}{4} f_e^o\right) O_2 + (f_e^o + f_s^o - 1) H^+$ $- \left(f_s^o \frac{1}{d}\right) C_nH_aO_bN_c + \left(f_s^o \frac{n-c}{d} - \frac{1}{7}\right) CO_2 + \left(f_s^o \frac{c}{d} - \frac{1}{7}\right) HCO_3^- + \left(\frac{3}{7} - \frac{1}{2} f_e^o - f_s^o \frac{2n-b+c}{d}\right) H_2O$
II(a)	$\left(\frac{1}{14}\right) C_4H_4O_4^{2-} + \left(f_s^o \frac{c}{d} - \frac{1}{8} f_e^o\right) NH_4^+ + \left(\frac{1}{8} f_e^o\right) NO_3^- + \left(\frac{5}{4} f_e^o + f_s^o - 1\right) H^+$ $- \left(f_s^o \frac{1}{d}\right) C_nH_aO_bN_c + \left(f_s^o \frac{n-c}{d} - \frac{1}{7}\right) CO_2 + \left(f_s^o \frac{c}{d} - \frac{1}{7}\right) HCO_3^- + \left(\frac{3}{7} - \frac{3}{8} f_e^o - f_s^o \frac{2n-b+c}{d}\right) H_2O$
III(b)	$\left(\frac{1}{14}\right) C_4H_4O_4^{2-} + \left(f_s^o \frac{c}{d}\right) NH_4^+ + \left(\frac{1}{2} f_e^o\right) NO_3^- - \left(\frac{1}{2} f_e^o\right) NO_2^- + (f_e^o + f_s^o - 1) H^+$ $- \left(f_s^o \frac{1}{d}\right) C_nH_aO_bN_c + \left(f_s^o \frac{n-c}{d} - \frac{1}{7}\right) CO_2 + \left(f_s^o \frac{c}{d} - \frac{1}{7}\right) HCO_3^- + \left(\frac{3}{7} - \frac{1}{2} f_e^o - f_s^o \frac{2n-b+c}{d}\right) H_2O$
IV(b)	$\left(\frac{1}{14}\right) C_4H_4O_4^{2-} + \left(f_s^o \frac{c}{d}\right) NH_4^+ + (f_e^o) NO_2^- - (f_e^o) NO + (2f_e^o + f_s^o - 1) H^+$ $- \left(f_s^o \frac{1}{d}\right) C_nH_aO_bN_c + \left(f_s^o \frac{n-c}{d} - \frac{1}{7}\right) CO_2 + \left(f_s^o \frac{c}{d} - \frac{1}{7}\right) HCO_3^- + \left(\frac{3}{7} - f_e^o - f_s^o \frac{2n-b+c}{d}\right) H_2O$
V(b)	$\left(\frac{1}{14}\right) C_4H_4O_4^{2-} + \left(f_s^o \frac{c}{d}\right) NH_4^+ + (f_e^o) NO - \left(\frac{1}{2} f_e^o\right) N_2O + (f_e^o + f_s^o - 1) H^+$ $- \left(f_s^o \frac{1}{d}\right) C_nH_aO_bN_c + \left(f_s^o \frac{n-c}{d} - \frac{1}{7}\right) CO_2 + \left(f_s^o \frac{c}{d} - \frac{1}{7}\right) HCO_3^- + \left(\frac{3}{7} - \frac{1}{2} f_e^o - f_s^o \frac{2n-b+c}{d}\right) H_2O$
VI(b)	$\left(\frac{1}{14}\right) C_4H_4O_4^{2-} + \left(f_s^o \frac{c}{d}\right) NH_4^+ + \left(\frac{1}{2} f_e^o\right) N_2O - \left(\frac{1}{2} f_e^o\right) N_2 + (f_e^o + f_s^o - 1) H^+$ $- \left(f_s^o \frac{1}{d}\right) C_nH_aO_bN_c + \left(f_s^o \frac{n-c}{d} - \frac{1}{7}\right) CO_2 + \left(f_s^o \frac{c}{d} - \frac{1}{7}\right) HCO_3^- + \left(\frac{3}{7} - \frac{1}{2} f_e^o - f_s^o \frac{2n-b+c}{d}\right) H_2O$

C_nH_aO_bN_c is the general empirical chemical formula of cells, where the coefficients n, a, b and c are the molar relationship between the elements: carbon, hydrogen, oxygen and nitrogen, respectively. Also, $d = (4n + a - 2b - 3c)$. fe^o and fs^o are the portion of electrons for coupling energy between catabolic and anabolic process according to TEEM2 [22, 74]. NH₄⁺ is the N-source for biomass synthesis. When the coefficient is evaluated if the result is positive indicates “reaction reactant” and if is negative indicates “reaction product”.

Table 3. Microbial Metabolic Reactions for individual mass degradation to reduce cytotoxic products NO or N₂O in anaerobic phase according to TEEM2 [22, 74].

NO	$\left(\frac{1}{d}\right) C_n H_a O_b N_c + (1)NO - \left(\frac{1}{2}\right) N_2O - \left(\frac{c}{d}\right) NH_4^+ - \left(\frac{n-c}{d}\right) CO_2 - \left(\frac{c}{d}\right) HCO_3^- + \left(\frac{2n-b+c}{d} - \frac{1}{2}\right) H_2O$
N ₂ O	$\left(\frac{1}{d}\right) C_n H_a O_b N_c + \left(\frac{1}{2}\right) N_2O - \left(\frac{1}{2}\right) N_2 - \left(\frac{c}{d}\right) NH_4^+ - \left(\frac{n-c}{d}\right) CO_2 - \left(\frac{c}{d}\right) HCO_3^- + \left(\frac{2n-b+c}{d} - \frac{1}{2}\right) H_2O$

C_nH_aO_bN_c is the general empirical chemical formula of cells, where the coefficients n, a, b and c are the molar relationship between the elements: carbon, hydrogen, oxygen and nitrogen, respectively. Also, $d = (4n + a - 2b - 3c)$. When the coefficient is evaluated if the result is positive indicates “reaction reactant” and if is negative indicates “reaction product”.

Table 4. Microbial metabolic reactions that represent aerobic^(a) and anaerobic^(b) pathways for the denitrifying bacterium *Paracoccus denitrificans* for individual-mass synthesis using different values of energy-transfer-efficiency (ϵ) according to TEEM2 [74] used for test INDISIM-Denitrification model [46].

I ^(a)	$(C_4H_4O_4)^{2-} + 0.66 NH_4^+ + 0.79 O_2 =$ $0.89 C_3H_{5,4}O_{1,45}N_{0,75} + 0.01 CO_2 + 1.34 HCO_3^- + 0.27 H_2O$	$\epsilon=0.84$
II ^(a)	$(C_4H_4O_4)^{2-} + 0.08 NH_4^+ + 0.52 NO_3^- + 1.05 H^+ + 0.18 H_2O =$ $0.80 C_3H_{5,4}O_{1,45}N_{0,75} + 0.20 CO_2 + 1.4 HCO_3^-$	$\epsilon=0.90$
III ^(b)	$(C_4H_4O_4)^{2-} + 0.30 NH_4^+ + 4.56 NO_3^- =$ $4.56 NO_2^- + 0.4 C_3H_{5,4}O_{1,45}N_{0,75} + 1.10 CO_2 + 1.70 HCO_3^- + 0.67 H_2O$	$\epsilon=0.41$
IV ^(b)	$(C_4H_4O_4)^{2-} + 0.57 NH_4^+ + 4.67 NO_2^- + 4.67 H^+ =$ $4.67 NO + 0.76 C_3H_{5,4}O_{1,45}N_{0,75} + 0.30 CO_2 + 1.43 HCO_3^- + 2.71 H_2O$	$\epsilon=0.84$
V ^(b)	$(C_4H_4O_4)^{2-} + 0.58 NH_4^+ + 4.60 NO =$ $2.30 N_2O + 0.77 C_3H_{5,4}O_{1,45}N_{0,75} + 0.27 CO_2 + 1.42 HCO_3^- + 0.37 H_2O$	$\epsilon=0.56$
VI ^(b)	$(C_4H_4O_4)^{2-} + 0.58 NH_4^+ + 2.29 N_2O =$ $2.29 N_2 + 0.77 C_3H_{5,4}O_{1,45}N_{0,75} + 0.27 CO_2 + 1.42 HCO_3^- + 0.37 H_2O$	$\epsilon=0.53$

I^(a) represents the pathway: Aerobic respiration, II^(a) represents the pathway: Nitrate Reduction - Dissimilatory in aerobic phase, and gathering the reactions III^(b), IV^(b), V^(b) and VI^(b) the pathway: Nitrate Reduction - Denitrification, all of them are represented according to Caspi et al., (2012); Knowles, (1982) and Zumft, (1997).

Table 5. Microbial metabolic reactions for individual mass degradation to reduce cytotoxic products NO and/or N₂O in anaerobic phase. For the denitrifying bacterium *Paracoccus denitrificans*, used for test INDISIM-Denitrification model [46].

NO	$\text{C}_3\text{H}_{5,4}\text{O}_{1,45}\text{N}_{0,75} + 12.25 \text{NO} =$ $6.125 \text{N}_2\text{O} + 0.75 \text{NH}_4^+ + 2.25 \text{CO}_2 + 0.75 \text{HCO}_3^- + 0.825 \text{H}_2\text{O}$
N ₂ O	$\text{C}_3\text{H}_{5,4}\text{O}_{1,45}\text{N}_{0,75} + 6.125 \text{N}_2\text{O} =$ $6.125 \text{N}_2 + 0.75 \text{NH}_4^+ + 2.25 \text{CO}_2 + 0.75 \text{HCO}_3^- + 0.825 \text{H}_2\text{O}$

733

Table 6. Microbial metabolic reactions that represent aerobic^(a) and anaerobic^(b) pathways for the denitrifying bacterium *Achromobacter xyloxidans*, for individual-mass synthesis using different values of energy-transfer-efficiency (ϵ) according to TEEM2 [74] used for test INDISIM-Denitrification model [46].

I ^(a)	$(C_4H_4O_4)^{2-} + 0.50 NH_4^+ + 0.89 O_2 =$ $0.50 C_5H_9O_{2.5}N + 0.01 CO_2 + 1.50 HCO_3^- + 0.01 H_2O$	$\epsilon = 0.76$
II ^(a)	$(C_4H_4O_4)^{2-} + 0.52 H_2O + 0.77 NO_3^- + 1.54 H^+ =$ $0.37 C_5H_9O_{2.5}N + 0.51 CO_2 + 1.63 HCO_3^- + 0.40 NH_4^+$	$\epsilon = 0.65$
III ^(b)	$(C_4H_4O_4)^{2-} + 0.24 NH_4^+ + 4.49 NO_3^- =$ $4.49 NO_2^- + 0.24 C_5H_9O_{2.5}N + 1.05 CO_2 + 1.76 HCO_3^- + 0.52 H_2O$	$\epsilon = 0.41$
IV ^(b)	$(C_4H_4O_4)^{2-} + 0.45 NH_4^+ + 4.54 NO_2^- + 4.54 H^+ =$ $4.54 NO + 0.45 C_5H_9O_{2.5}N + 0.20 CO_2 + 1.55 HCO_3^- + 2.37 H_2O$	$\epsilon = 0.84$
V ^(b)	$(C_4H_4O_4)^{2-} + 0.50 NH_4^+ + 3.53 NO =$ $1.77 N_2O + 0.50 C_5H_9O_{2.5}N + 0.01 CO_2 + 1.50 HCO_3^- + 0.003 H_2O$	$\epsilon = 0.66$
VI ^(b)	$(C_4H_4O_4)^{2-} + 0.24 NH_4^+ + 4.50 N_2O =$ $4.50 N_2 + 0.24 C_5H_9O_{2.5}N + 1.05 CO_2 + 1.76 HCO_3^- + 0.52 H_2O$	$\epsilon = 0.27$

I^(a) represents the pathway: Aerobic respiration, II^(a) represents the pathway: Nitrate Reduction - Dissimilatory in aerobic phase, and gathering the reactions III^(b), IV^(b), V^(b) and VI^(b) the pathway: Nitrate Reduction - Denitrification, all of them are represented according to Caspi et al., (2012); Knowles, (1982) and Zumft, (1997).

Table 7. Microbial metabolic reactions for individual mass degradation to reduce cytotoxic products NO and/or N₂O in anaerobic phase. For the denitrifying bacterium *Achromobacter xyloxidans*, used for test INDISIM-Denitrification model [46].

NO	$C_5H_9O_{2.5}N + 21 NO = 10.5 N_2O + NH_4^+ + 4 CO_2 + HCO_3^- + 2 H_2O$
N ₂ O	$C_5H_9O_{2.5}N + 10.5 N_2O = 10.5 N_2 + NH_4^+ + 4 CO_2 + HCO_3^- + 2 H_2O$

735

Table 8. Uptake-rate (u_i) parameter's values with units ($\text{mol}_{\text{nutrient}} \cdot \text{C} \cdot \text{mol}_{\text{mic}}^{-1} \cdot \text{h}^{-1}$) for the sensitivity analysis of the uptake-rate (u_i) parameter for denitrifying bacterium *P. denitrificans* used for test INDISIM-Denitrification model [46].

Nutrient	Uptake-rate ($\text{mol}_{\text{nutrient}} \cdot \text{C} \cdot \text{mol}_{\text{mic}}^{-1} \cdot \text{h}^{-1}$)		
	Testing values		
	Low (L)	Medium (M)	High (H)
Succinate	0.051	0.102	0.204 ^a
Ammonium	-----	-----	0.105 ^a
Oxygen	-----	-----	0.125 ^a
Nitrate-a (aerobic)	0.000911	0.00911	0.0911 ^a
Nitrate-x (anaerobic)	0.00398	0.0398	0.398 ^{a,b}
Nitrite	0.00214	0.0214	0.214 ^{a,b}
Nitric Oxide	0.00209	0.0209	0.209 ^{a,b}
Nitrous Oxide	0.00104	0.0104	0.104 ^{a,b}

The values (a) are the result of performing calculations between the maximum growth rate ($\mu_{\text{max}} = 0.418 \text{ h}^{-1}$, van Verseveld et al., 1983) and the stoichiometric coefficients of each metabolic reaction adjusted by TEEM2 (Table 4). The values (b) are the result of dividing each high uptake-rate by 4 due to the maximum growth rate being achieved when the four reactions (III^(b), IV^(b), V^(b) and VI^(b)) are carried out by the bacterium.

Table 9. Uptake-rate (u_i) parameter's values with units ($\text{mol}_{\text{nutrient}} \cdot \text{C} \cdot \text{mol}_{\text{mic}}^{-1} \cdot \text{h}^{-1}$) used in the sensitivity analysis of this parameter for denitrifying bacterium *A. xylosoxidans* used for test INDISIM-Denitrification model [46].

Nutrient	Uptake-rate ($\text{mol}_{\text{nutrient}} \cdot \text{C} \cdot \text{mol}_{\text{mic}}^{-1} \cdot \text{h}^{-1}$)		
	Testing values		
	Low (L)	Medium (M)	High (H)
Succinate	0.036	0.072	0.144 ^a
Ammonium	-----	-----	0.050 ^a
Oxygen	-----	-----	0.089 ^a
Nitrate-a (aerobic)	0.001031	0.01031	0.1031 ^a
Nitrate-x (anaerobic)	0.00235	0.0235	0.235 ^{a,b}
Nitrite	0.00126	0.0126	0.126 ^{a,b}
Nitric Oxide	0.00089	0.0089	0.089 ^{a,b}
Nitrous Oxide	0.00236	0.0236	0.236 ^{a,b}

The values (a) are the result of performing calculations between the maximum growth rate ($\mu_{\text{max}} = 0.250 \text{ h}^{-1}$, Nielsen et al., 2006) and the stoichiometric coefficients of each metabolic reaction adjusted by TEEM2 (Table 6). The values (b) are the result of dividing each high uptake-rate by 4 due to the maximum growth rate being achieved when the four reactions (III^(b), IV^(b), V^(b) and VI^(b)) are carried out by the bacterium.

Table 10. Values used in the sensitivity analysis performed with the parameter for cellular maintenance and individual mass degradation coefficient, for two denitrifying bacteria (*P. denitrificans* and *A. xylosoxidans*) used for test INDISIM-Denitrification model [46].

Cellular maintenance ($gC_{\text{donor}} \cdot gC_{\text{mic}}^{-1} \cdot h^{-1}$)	2.0×10^{-3} (a)	4.0×10^{-3}	2.0×10^{-2}	4.0×10^{-2}
Mass degradation (h^{-1})	2.2×10^{-2} (a)	4.0×10^{-2}	6.0×10^{-2}	8.5×10^{-2}

(a) Reference value obtained from initial model calibration.

Table 11. INDISIM-Denitrification model parameters values for *P. denitrificans* [46].

Nutrient	Culture medium initial concentration [mM] Felgate et al. (2012)	Availability coefficient – a_i (h ⁻¹) fixed according to Dab	Uptake-rate – u_i – (mol _{nutrient} ·C·mol _{mic} ⁻¹ ·h ⁻¹)
Succinate	5 ^c – 20 ^d	0.28 ^{a,b}	0.204 ^{a,b}
Ammonium	10 ^{c,d}	0.84 ^{a,b}	0.105 ^{a,b}
Oxygen	0.236 ^{c,d}	0.79 ^{a,b}	0.125 ^a
Nitrate-a (aerobic)	4.9983 ^d – 21.6095 ^c	0.63 ^{a,b}	0.00911 ^a
Nitrate-x (anaerobic)			0.039 ^b
Nitrite	0.0255 ^c – 0.0112 ^d	0.78 ^{a,b}	0.214 ^b
Nitric Oxide	-----	1.00 ^{a,b}	0.209 ^b
Nitrous Oxide	0.003 ^c – 0.000028 ^d	0.50 ^{a,b}	0.104 ^b
Other bacterial parameters			
Parameter	Calibrated value	Reference	
Cellular maintenance coefficient (gC _{donor} ·gC _{mic} ⁻¹ ·h ⁻¹)	0.0020 ^{a,b}	Gras et al. (2011)	
Mass degradation coefficient (h ⁻¹)	0.022	Calibrated	
Mass split	0.50 (15% coefficient of variation)	Derived from [66]	
Small bacterium size (µm)	0.5 ^{a,b}	Holt et al. (1994)	
Big bacterium size (µm)	0.9 ^{a,b}		
Minimum bacterium size at reproduction	75% of big bacterium size (15% coefficient of variation)	Derived from [68] and [66]	

Phase: (a) Aerobic, (b) Anaerobic. Experiment: (c) Succinate-limited/NO₃⁻-sufficient, (d) Succinate-sufficient/NO₃⁻-limited.

Table 12. INDISIM-Denitrification model parameters values for A xylooxidans [46].

Nutrient	Culture medium initial concentration [mM] Felgate et al. (2012)	Availability coefficient – a_i (h^{-1}) fixed according to Dab	Uptake-rate – u_i – ($mol_{nutrient} \cdot C \cdot mol_{mic}^{-1} \cdot h^{-1}$)
Succinate	5 ^c – 20 ^d	0.28 ^{a,b}	0.144 ^{a,b}
Ammonium	10 ^{c,d}	0.84 ^{a,b}	0.050 ^{a,b}
Oxygen	0.236 ^{c,d}	0.79 ^{a,b}	0.089 ^a
Nitrate-a (aerobic)	5.1538 ^d – 21.7469 ^c	0.63 ^{a,b}	0.01031 ^a
Nitrate-x (anaerobic)			0.235 ^b
Nitrite	0.00765 ^c – 0.36863 ^d	0.77 ^{a,b}	0.00126 ^b
Nitric Oxide	-----	1.00 ^{a,b}	0.0089 ^b
Nitrous Oxide	0.00001818 ^c – 0.00006263 ^d	0.50 ^{a,b}	0.236 ^b
Other bacterial parameters			
Parameter	Calibrated value	Reference	
Cellular maintenance coefficient ($gC_{donor} \cdot gC_{mic}^{-1} \cdot h^{-1}$)	0.0020 ^{a,b}	Gras et al. (2011)	
Mass degradation coefficient (h^{-1})	0.085	Calibrated	
Mass split	0.50 (15% coefficient of variation)	Derived from [66]	
Smallest bacterium size (μm)*	0.63 ^{a,b}	Holt et al. (1994)	
Big Biggest bacterium size (μm)*	1.40 ^{a,b}		
Minimum bacterium size at reproduction	75% of big bacterium size (15% coefficient of variation)	Derived from [68] and [66]	

Phase: (a) Aerobic, (b) Anaerobic. Experiment: (c) Succinate-limited/ NO_3^- -sufficient, (d) Succinate-sufficient/ NO_3^- -limited. (*) This size refers to a spherical equivalent diameter.

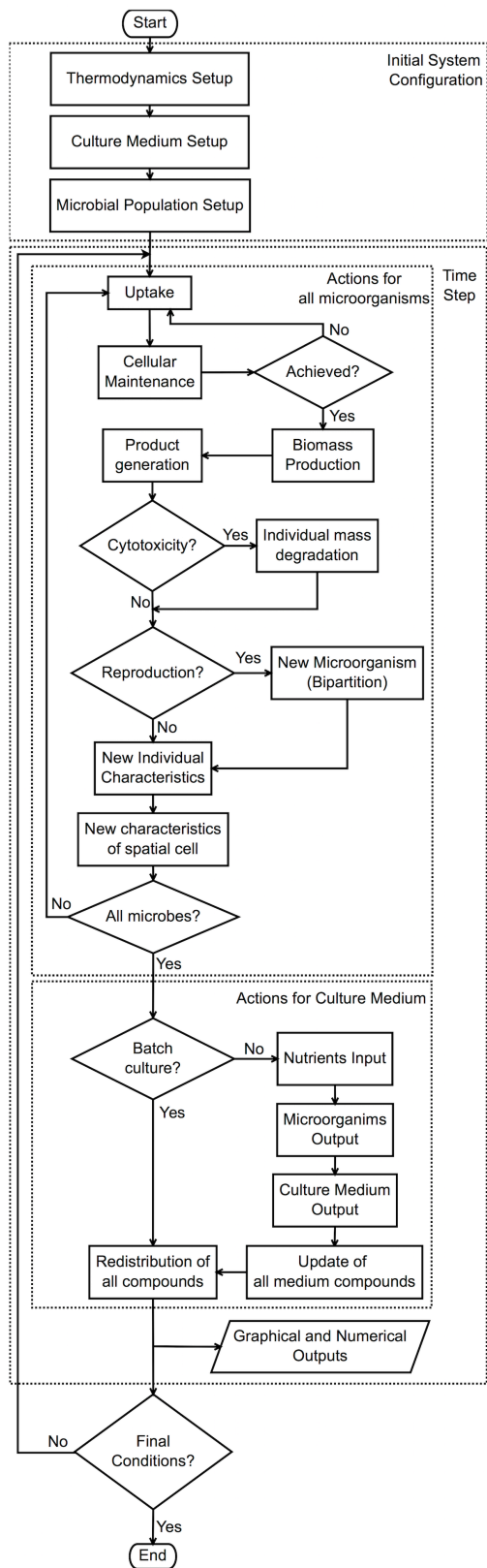


Figure 1. Schematic diagram of the INDISIM-Denitrification model [46].

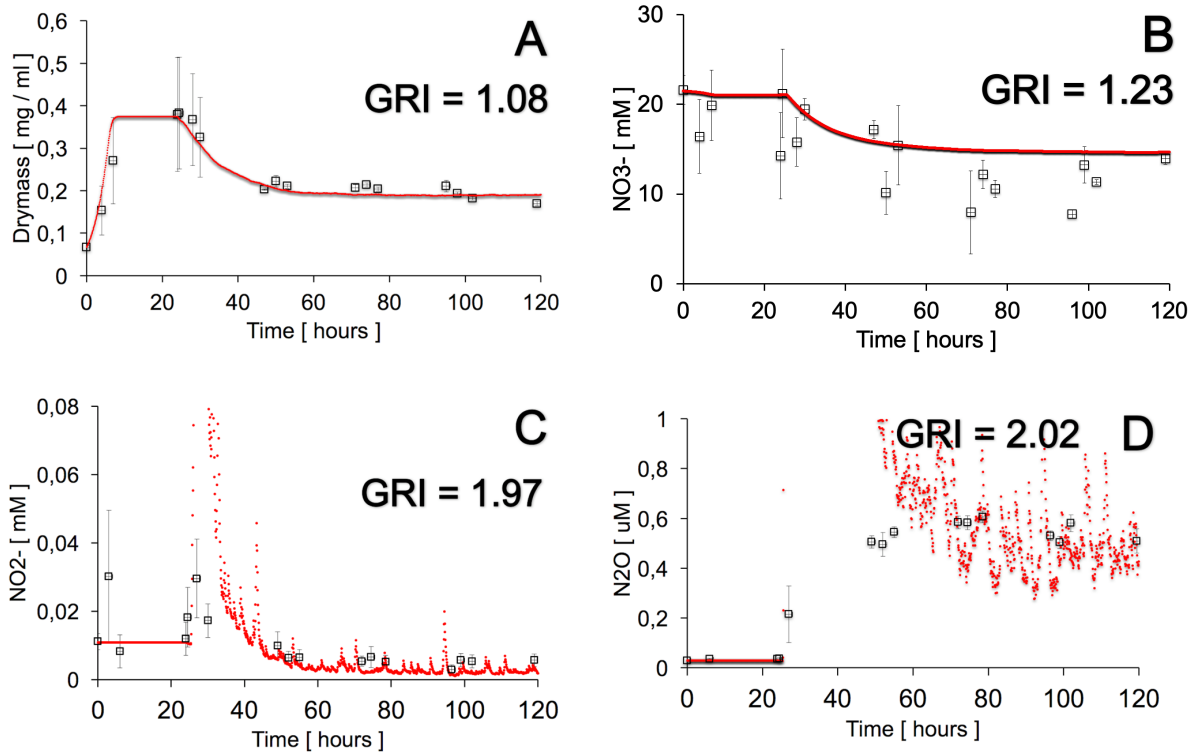


Figure 3. INDISIM-Denitrification simulation results using the empirical chemical formula of *Paracoccus denitrificans* (dots and continuous line) and experimental values (squares) are presented with their standard error [18] for the experiment E1: succinate-limited/NO₃-sufficient. Temporal evolution of biomass (A), nitrate (B), nitrite (C) and nitrous oxide (D) in aerobic and anaerobic phases. The simulation results are compared with the experimental values through GRI (Geometric Reliability Index).

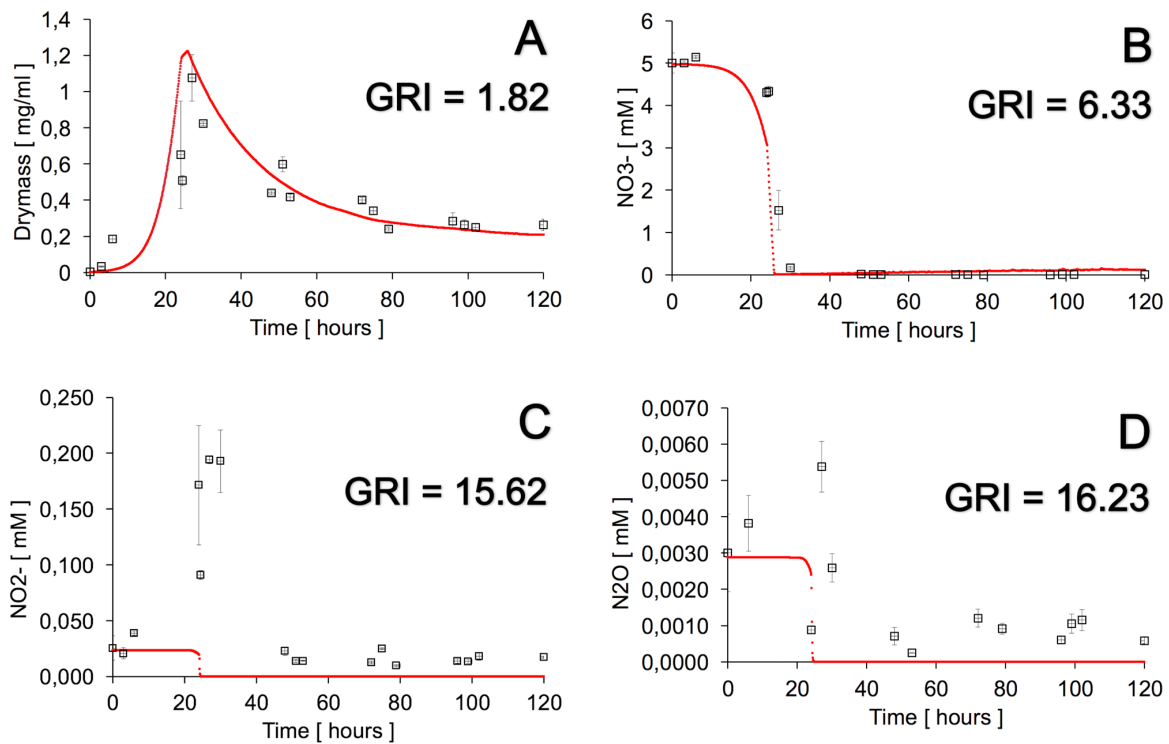


Figure 4. INDISIM-Denitrification simulation results using the empirical chemical formula of *Paracoccus denitrificans* (dots and continuous line) and experimental values (squares) are presented with their standard error [18] for the experiment E2: succinate-sufficient/NO₃⁻-limited. Temporal evolution of biomass (A), nitrate (B), nitrite (C) and nitrous oxide (D) in aerobic and anaerobic phases. The simulation results are compared with the experimental values through GRI (Geometric Reliability Index).

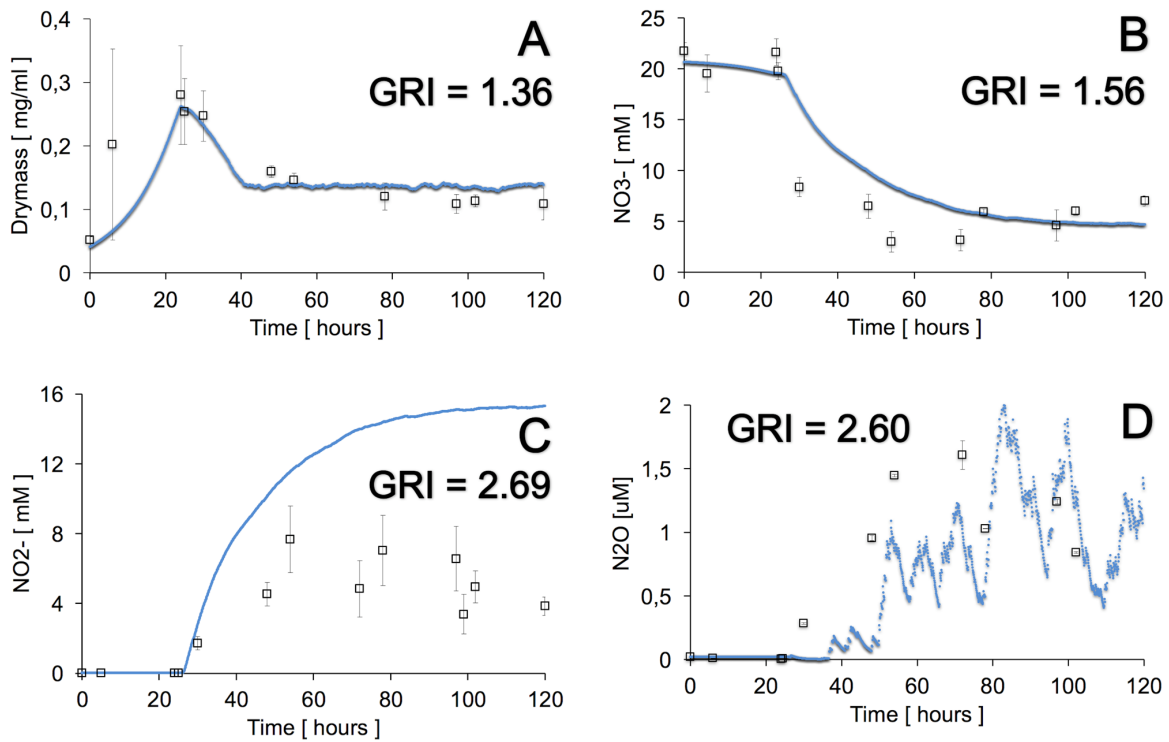


Figure 5. INDISIM-Denitrification simulation results using the empirical chemical formula of *Achromobacter xylosoxidans* (dots and continuous line) and experimental values (squares) are presented with their standard error [18] for the experiment E1: succinate-limited/NO₃⁻-sufficient. Temporal evolution of biomass (A), nitrate (B), nitrite (C) and nitrous oxide (D) in aerobic and anaerobic phases. The simulation results are compared with the experimental values through GRI (Geometric Reliability Index).

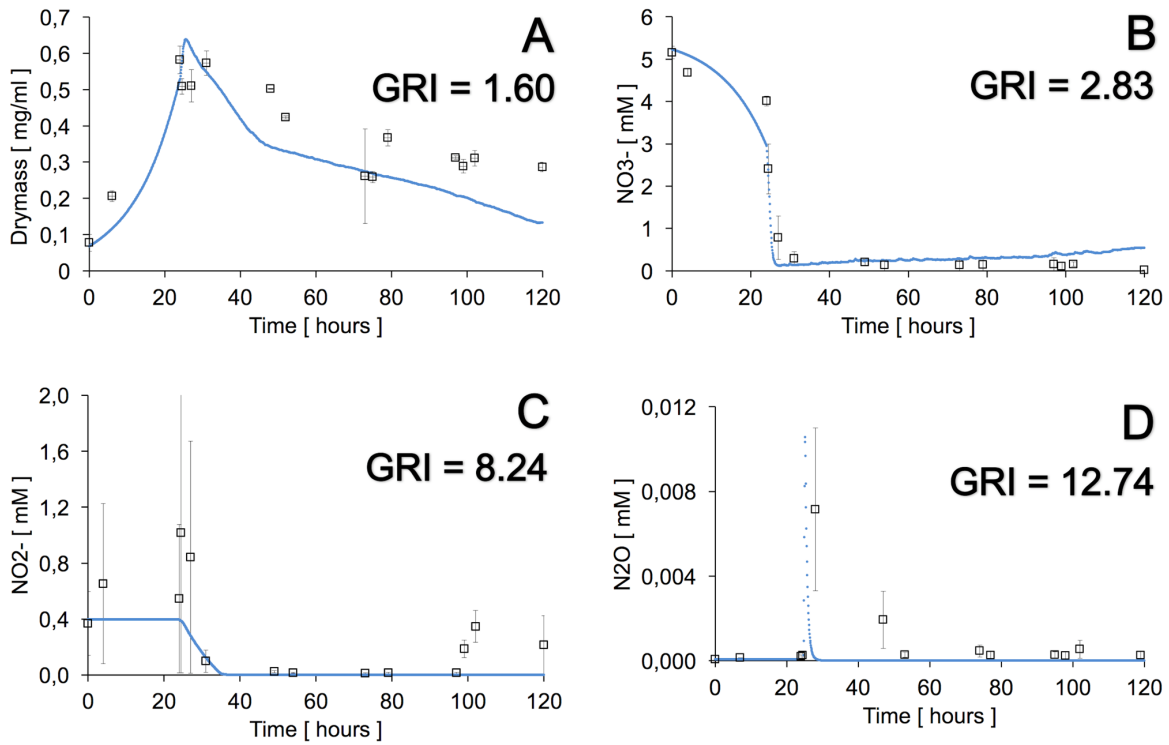


Figure 6. INDISIM-Denitrification simulation results using the empirical chemical formula of *Achromobacter xylooxidans* (dots and continuous line) and experimental values (squares) are presented with their standard error [18] for the experiment E2: succinate-sufficient/NO₃⁻-limited. Temporal evolution of biomass (A), nitrate (B), nitrite (C) and nitrous oxide (D) in aerobic and anaerobic phases. The simulation results are compared with the experimental values through GRI (Geometric Reliability Index).

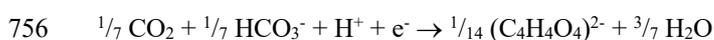
748 Supplementary Material

749 Section I. Cellular maintenance

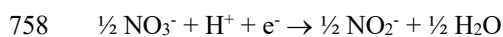
750 Before biomass synthesis, each individual in INDISIM-Denitrification model executes a behavior-rule for cellular
 751 maintenance. For example to fit the individual behavior-rule for the first reaction in the anaerobic phase we employ an
 752 appropriate maintenance requirement for heterotrophic microorganisms of $0.002 \text{ gCdonor} \cdot \text{gCmicrobial}^{-1} \cdot \text{h}^{-1}$ proposed by
 753 Gras et al., (2011), and the energy reaction (Re) between succinate and nitrate:

754 **Step 1.** Write inorganic and organic half-reactions for e-donor and e-acceptor.

755 E-donor (succinate) half-reaction (Rd):



757 E-acceptor (nitrate) half-reaction (Ra):



759 **Step 2.** According to [2] following the equation ($\text{Re} = \text{Ra} - \text{Rd}$) a balanced stoichiometric equation can be written for this
 760 energy reaction as follows.



761 Re is the balanced chemical equation for the energy reaction to fit the individual behavior-rule for aerobic maintenance
 762 in INDISIM-Denitrification model.

763 **Step 3.** Computation of specific maintenance requirements for the first reaction in anaerobic phase each step time using
 764 the elementary cell composition for *P. denitrificans* ($\text{C}_3\text{H}_{5.4}\text{N}_{0.75}\text{O}_{1.45}$) proposed by [3, 4].

$$765 \quad 0.002 \frac{\text{gC}_{\text{succinate}}}{\text{gC}_{\text{microbial}} \cdot \text{h}} \times \frac{1 \text{ mol Succinate}}{48 \text{gC}_{\text{succinate}}} \times \frac{36 \text{gC}_{\text{microbial}}}{1 \text{ mol Biomass}} \times \frac{0.08333 \text{ h}}{\text{step time}} = 0.000125 \frac{\text{mol Succinate}}{\text{mol Biomass} \cdot \text{step time}}$$

$$766 \quad 0.000125 \frac{\text{mol Succinate}}{\text{mol Biomass} \cdot \text{step time}} \times \frac{0.50 \text{ mol NO}_3^-}{0.0714 \text{ mol succinate}} = 0.000875 \frac{\text{mol NO}_3^-}{\text{mol Biomass} \cdot \text{step time}}$$

767 **Step 4.** Maintenance requirements computation, for the first reaction in anaerobic phase each step, according to the
 768 individual mass. Consider an individual who has a diameter of $0.9 \mu\text{m}$ (individual mass of 6 pmol approximately).

$$769 \quad 0.000125 \frac{\text{mol Succinate}}{\text{mol Biomass} \cdot \text{step time}} \times 6 \text{ pmol biomass} = 0.00075 \text{ pmol Succinate}$$

$$770 \quad 0.000875 \frac{\text{pmol NO}_3^-}{\text{pmol Biomass} \cdot \text{step time}} \times 6 \text{ pmol biomass} = 0.00525 \text{ pmol NO}_3^-$$

771 Then the individual compares these quantities to the corresponding uptakes and picks the lowest values to execute the
 772 energy reaction. First establish which is the reactant limiting, with this information run the reaction and finally update the

773 corresponding uptakes.

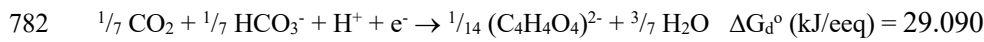
774

775 **Section II. Biomass generation**

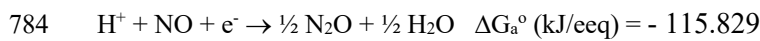
776 Example of calculations for anaerobic nitric oxide reduction with succinate as e-donor and C-source, ammonium as N-
 777 source and nitric oxide as e-acceptor with $e = 0.56$, to fit the individual behavior-rule for biomass generation in INDISIM-
 778 Denitrification model for the reaction ($\text{NO} \rightarrow \text{N}_2\text{O}$) in metabolic pathway 3.

779 **Step 1.** Write inorganic and organic half-reactions and their Gibb's standard free energy at pH = 7.0 according to Rittmann
 780 and McCarty (2001) for e-donor, e-acceptor and cell synthesis reaction with ammonium as N-source.

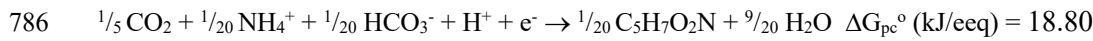
781 E-donor (succinate) $\frac{1}{2}$ reaction (R_d):



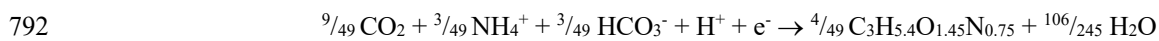
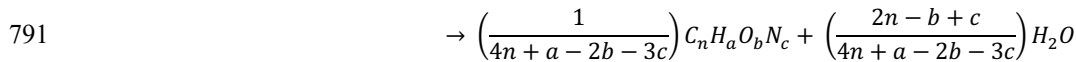
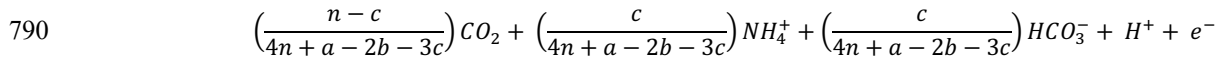
783 E-acceptor (nitric oxide) $\frac{1}{2}$ reaction (R_a):



785 Cell $\frac{1}{2}$ reaction (R_c) with ammonium as N-source:

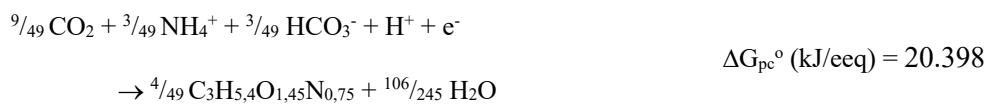


787 **Step 2.** Adjust the cell $\frac{1}{2}$ reaction (R_c) to *P. denitrificans* elementary cell composition $\text{C}_3\text{H}_{5.4}\text{N}_{0.75}\text{O}_{1.45}$ (van Verseveld et
 788 al., 1979, 1983) following the methodology proposed by Rittmann and McCarty (2001). Where, $n = 3$, $a = 5.4$, $b = 0.75$
 789 and $c = 1.45$.



793
$$18.80 \frac{\text{kJ}}{\text{eeq}} \times \frac{20 \text{ eeq}}{1 \text{ mol C}_5\text{H}_7\text{O}_2\text{N}} \times \frac{1 \text{ mol C}_5\text{H}_7\text{O}_2\text{N}}{113.11 \text{ g}_{\text{microbial}}} \times \frac{75.17 \text{ g}_{\text{microbial}}}{1 \text{ mol C}_3\text{H}_{5.4}\text{O}_{1.45}\text{N}_{0.75}} \times \frac{1 \text{ mol C}_3\text{H}_{5.4}\text{O}_{1.45}\text{N}_{0.75}}{49/4 \text{ eeq}} = 20.398 \frac{\text{kJ}}{\text{eeq}}$$

794 For *P. denitrificans* elementary cell composition the cell $\frac{1}{2}$ reaction (R_c) with ammonium as N-source with Gibb's
 795 standard free energy at pH = 7.0 is



796 **Step 3.** Degree of reduction computation for e-donor and cells:

797
$$\gamma_d = \frac{\text{electrons donor}}{\text{Carbon donor}} = \frac{14}{4} = 3.5$$

798
$$\gamma_x = \frac{\text{electron cells}}{\text{Carbon cells}} = \frac{49/4}{3} = 4.083$$

799 **Step 4.** Computation of f_s° , f_e° and $Y_{c/e}$ according to McCarty (2007).

$$800 \quad A = -\frac{\Delta G_s}{\varepsilon \Delta G_e} = \frac{\frac{(\Delta G_{fa} - \Delta G_d)}{\varepsilon^m} + \frac{(\Delta G_{in} - \Delta G_{fa})}{\varepsilon^n} + \frac{\Delta G_{pc}}{\varepsilon}}{\varepsilon \left(\Delta G_a - \Delta G_d - \frac{q}{p} \Delta G_{xy} \right)} = \frac{f_e^o}{f_s^o}$$

801 $\Delta G_{in} = 30.90$ kJ/eqq. Since no oxygenase is involved, $q = 0$. Since succinate is not a C1 compound, $\Delta G_{fa} = 0$ and $m = n$.

802 Since $(\Delta G_{in} - \Delta G_d) > 0 \rightarrow (30.9 - 29.09) > 0$, $n = 1$, $m = 1$. Using $e = 0.41$, and if standard conditions apply.

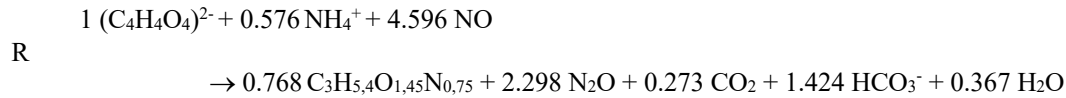
$$803 \quad A = -\frac{\frac{(0 - 29.09)}{0.56^1} + \frac{(30.90 - 0)}{0.56^1} + \frac{20.398}{0.56}}{0.56(-115.829 - 29.09 - 0)} = 0.489$$

$$804 \quad f_s^o = \frac{1}{1 + A} = \frac{1}{1 + 0.489} = 0.672$$

$$805 \quad f_e^o = A \cdot f_s^o = 0.489 \times 0.672 = 0.328$$

$$806 \quad Y_{C/C} = \frac{\gamma_d}{\gamma_x} f_s^o = \frac{3.5}{4.083} \times 0.672 = 0.576 \left[\frac{\text{mol } C_{\text{cells}}}{\text{mol } C_{\text{succinate}}} \right]$$

807 **Step 5.** A balanced stoichiometric equation can then be written. The overall reaction R is equal to $R = f_e^o R_a + f_s^o R_c - R_d$
 808 according to Rittmann and McCarty (2001) and the coefficients present on Table III for one mole of succinate we can
 809 write.



810 **R** is the balanced chemical equation using the Thermodynamic Electron Equivalents Model second version to fit the
 811 individual behavior-rule for biomass generation in INDISIM-Denitrification model for metabolic pathway ($\text{NO} \rightarrow \text{N}_2\text{O}$).

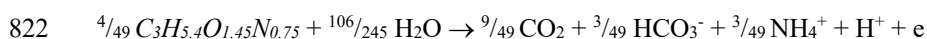
812

813 **Section III. Individual mass degradation to reduce cytotoxic products**

814 To develop the new individual behaviour-rule to reduce the concentration of cytotoxic products (NO and/or N₂O), the
 815 individual mass will be used by the bacterium as e-donor when the C-source is a limiting substrate in the media. To obtain
 816 this new metabolic process in the context of IBM, the bacterial biomass of each individual diminishes; the biomass half-
 817 reaction acts as e-donor and is combined with the e-acceptor half-reaction, and the MMR that represents the individual
 818 mass degradation reaction can be written.

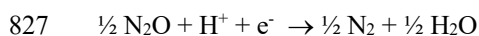
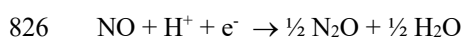
819 For instance, we take the bacterium *P. denitrificans* to show how to write this reaction.

820 **Step 1.** Considering the elementary cell composition for *P. denitrificans* (C₃H_{5.4}N_{0.75}O_{1.45}) [3, 4], the general biomass
 821 half-reaction equation [2] may be written as:

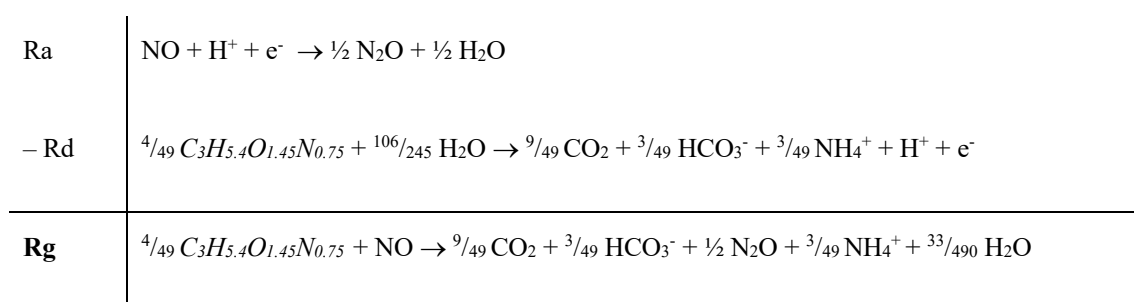


823 This reaction is the e-donor half-reaction (Rd) which considers the individual mass as electron source, breaking it down
 824 into CO₂, HCO₃⁻ and NH₄⁺. These electrons will be transferred to the e-acceptor.

825 **Step 2.** It is necessary to write the half-reactions for the e-acceptors considered, as follows:



828 **Step 3.** Following TEEM's methodology a balanced stoichiometric reaction can be written to represent the individual
 829 mass degradation to reduce cytotoxic products.



830 Therefore, Rg is the microbial metabolic reaction using TEEM to represent the individual mass degradation to reduce NO
 831 which will be a cytotoxic product.

832 **Step 4.** To write Rg in a standard way, we divide all of the stoichiometric coefficients by the e-donor coefficient (biomass).
 833 Taking into account this methodology and using different e-acceptors and the empirical cell composition of each
 834 bacterium, we can write the individual mass degradation reactions for both.

835

836 **Section IV. INDISIM-Denitrification model description**

837 To describe our model we use the ODD protocol (“Overview, Design concepts, and Details”), which helps to ensure that
838 the model description is complete [6–8].

839 **1 Purpose**

840 To develop a computational model for the denitrification process carried out by denitrifying bacteria growing in batch
841 and continuous culture, in aerobic and anaerobic growing conditions, and to reproduce a bioreactor experimental protocol.
842 To carry out the sensitivity analyses for the individual uptake parameters, the cellular maintenance, the individual mass
843 degradation coefficient for different culture media compositions.

844 **2 Entities, State Variables, and Scales**

845 The INDISIM-Denitrification model has two types of entities: individuals and square patches of culture medium. Each
846 individual represents a denitrifying bacterium and is identified by a number, its individual variables are: location (XY
847 grid cell coordinates of where it is), mass (molar units), reproduction mass (molar units), internal metabolic product
848 amounts (molar units) and counters for each metabolic reaction and reproduction cycle. To assign the initial mass, the
849 model assumes that each bacterium has spherical shape with a minimum and maximum diameter (μm) which is defined
850 by the user. The individual mass is then deduced from cell volume by assuming the microbial mass density equal to 1.1
851 $\text{g}\cdot\text{cm}^{-3}$, which has been used in previous INDISIM models [1].

852 A two-dimensional lattice of 25×25 grid cells represents the bioreactor that contains the culture medium; each cell
853 represents 1 nl, so that the total bioreactor volume is 625 nl.

854 Each spatial cell has a position identifier in XY coordinates, and the variables are: total amount (molar units) of each
855 nutrient, succinate, NH_4^+ , O_2 , NO_3^- , and metabolic products, NO_2^- , NO , N_2O , N_2 and CO_2 . All microbial and culture
856 medium processes are discretized in time steps. One time step represents 5 min; for the current work the simulations were
857 run for 1440 time steps (120 h) and normally with all of the fixed parameters one simulation takes 6 or 7 minutes (using
858 a desktop PC) and when you change all of the parameters of the model, for example, in the sensitivity analysis, one run
859 could takes 6-7 hours (using a desktop PC). The model variable outputs are: (a) the concentration of nutrients and
860 metabolic products (mM or μM) and dry biomass ($\text{mg}\cdot\text{ml}^{-1}$) in a text file, (b) a histogram to show the biomass distribution,
861 (c) a plot to show the frequency of use of each metabolic reaction, (d) all MMRs written using TEEM for any denitrifying
862 bacteria, and (e) numerical values of calculated GRI for four time evolutions: microbial biomass (dry mass), NO_3^- , NO_2^-
863 and N_2O .

864 **3 Process Overview and Scheduling**

865 The initial system configuration has three main aspects to consider: (a) thermodynamics setup, in which the empirical
866 chemical formula of the denitrifying bacterium is required and established by the user. All the MMRs for cellular
867 maintenance, individual-mass synthesis and individual-mass degradation to reduce cytotoxic products following the
868 TEEM methodology are written, (b) culture medium setup; the grid cells setup its values according to the experimental
869 protocols published by Felgate et al. (2012) and considering the experiment (E1 or E2) under study, and (c) microbial
870 population setup; the initial population setup its values considering the Felgate et al. (2012) population values, the bacteria
871 size, which is defined by the user and the empirical chemical formula for the denitrifying bacterium under study.

872 At each time step all of the individuals are controlled using a set of time-dependent variables for each bacterium. All
873 individuals have the opportunity to perform the following processes: nutrient uptake, cellular maintenance, individual
874 mass synthesis, individual mass degradation to reduce internal cytotoxic products, and bipartition.

875 Culture medium processes are different depending on the management bioreactor protocol, but in any case, the culture
876 medium is homogenized after some time steps to simulate chemostat agitation. At the beginning of the simulation the
877 bioreactor works as a batch culture with oxygen saturated conditions (236 μM), and the user can choose at what time to
878 end this phase, and switch to continuous culture in anaerobic conditions, with certain dilution rate that force the input and
879 output of culture media (with nutrients in the input and metabolic products and microorganisms in the output) according
880 to the dilution rate fixed by the user. For each time step the time-dependent variables of individuals and culture medium
881 are recalculated and the state variables changes are immediately assigned generating an asynchronous update, and then
882 the graphics and digital outputs are updated. Figure 1 shows the INDISIM-Denitrification schematic diagram.

883 **4 Design Concepts**

884 **4.1 Basic Principles**

885 The individual behavior-rules are: (a) nutrient uptake, (b) cellular maintenance, (c) growth when a microorganism
886 executes any of the metabolic reactions adjusted by TEEM (Table II), (d) individual mass degradation to reduce internal
887 cytotoxic products, and (e) cell division following binary fission. The system actions are those conducted by the general
888 chemostat procedures when it works as a batch culture with constant oxygenation or a continuous culture with a dilution
889 rate.

890 **4.2 Emergence**

891 Model outputs are the result of the interaction between individuals and the culture medium. The model is not forced to
892 reproduce the biomass evolution, nutrient depletion, metabolic and/or denitrification products generation, or other
893 patterns that appear at the system level.

894 **4.3 Adaptation**

895 All the individuals follow the same behavior-rules. Individuals act one after another, not in parallel. Hence, after one
896 individual carries out all of its actions the composition of the spatial cell where it lives changes and the next individual is
897 run within a different medium composition. In consequence, the metabolic pathway that it might follow could be different.
898 Before starting the individual actions, it is required to check the O_2 dissolved concentration in the culture medium: if the
899 O_2 dissolved in the spatial cell is lower than a threshold value (O_{2-MIN}) the bacterium uses the anaerobic metabolism and
900 otherwise it uses the aerobic metabolism. After that, the individual can perform cellular maintenance and mass synthesis
901 to growth in aerobic or anaerobic phase. The last metabolic action is to respond to the internal concentrations of cytotoxic
902 gases (NO and/or N_2O). This individual rule is executed only in the anaerobic phase and when the internal amount of the
903 e-donor (C-source); is not enough to execute the next reaction in the denitrification pathway and the internal amount of
904 cytotoxic products (NO and/or N_2O) are accessible in the bacterial cell. Then, the individual can degrade its own mass
905 and reduce it according to the MMRs presented in Table III. At the end of time-step the individual check whether to
906 divide or not, depending on whether or not it has reached the minimum reproduction mass.

907 NetLogo platform uses an explicit time scheme and a runtime approach that is not naturally parallelizable. Each time step,
908 NetLogo agents act sequentially following a randomly chosen order. Under these circumstances, the most immediate
909 updating scheme is the asynchronous implementation of the model, although a synchronous scheme is also achievable.
910 The asynchronous scheme has been considered as a good approximation of real continuous time [10–12]. The reader
911 should notice that the implementation of the model using a synchronous or asynchronous scheme could lead different
912 model outputs and diverse types of discrepancies with the reality being represented. This should be specifically taken into
913 account if the model is transferred or extended to other modeling frameworks.

914 **4.4 Interaction**

915 The denitrifying bacterium is the only bacteria species in the virtual bioreactor. The microorganisms interact with the
916 culture medium; therefore, there is an indirect interaction in which nutrient competition takes place among the bacteria
917 that share the same spatial cell.

918 **4.5 Collective**

919 Simulated microorganisms do not form aggregates; each individual acts uniquely.

920 **4.6 Stochasticity**

921 The reproduction threshold biomass for each bacterium is determined using a normal distribution, which has also been
922 used to generate the initial population biomasses. For the physical separation of the two bacteria the original mass is split
923 into two new bacteria with masses according to a value from normal random distribution. At each time step, each
924 individual nutrient uptake capacity for each nutrient is established from a normal random distribution with the mean value
925 and a standard deviation of 5% of this value. The dilution rate for each input-output is obtained by using the normal
926 random distribution with mean value $d = 0.05 \text{ h}^{-1}$ and standard deviation 0.0025, in order to represent the experimental
927 error. When the individual used the behavior-rule to reduce internal cytotoxic products, we consider that the bacterium
928 could determine the portion of its own biomass that will be degraded to reduce cytotoxic products according to a value
929 from the normal random distribution with mean value given by the mass degradation coefficient, with units (h^{-1}), and
930 standard deviation of 5% of this value. The initial culture medium composition and $\text{O}_2\text{-MIN}$ threshold value are established
931 from normal distributions with mean values determined by the experimental procedure [9] and standard deviations of 5%
932 of these values. When the simulation starts, each bacterium has a position randomly assigned in culture medium and this
933 position randomly changes at some time steps.

934 **4.7 Observation**

935 The graphical and numerical outputs of the model are (a) the concentration ($\text{mmol}\cdot\text{l}^{-1}$ or $\text{umol}\cdot\text{l}^{-1}$) of each culture medium
936 component (succinate, NH_4^+ , O_2 , NO_3^- , CO_2 , HCO_3^- , NO_2^- , NO , N_2O and N_2), (b) microbial biomass ($\text{mg}\cdot\text{ml}^{-1}$), the
937 population mass distribution, (c) a graphical view to show the frequency of use of each metabolic reaction, (d) all MMRs
938 written using TEEM for any denitrifying bacteria, and (e) GRI's values for four time evolutions: microbial biomass (dry
939 mass), NO_3^- , NO_2^- and N_2O .

940 At each time step (the user can obtain all simulated data in output file with extension “.txt”).

941 **5 Initialization**

942 The user can adjust: (a) the culture medium composition ($\text{mmol}\cdot\text{l}^{-1}$) of succinate, NH_4^+ , O_2 and NO_3^- , (b) $\text{O}_{2-\text{MIN}}$ value
943 which is in the range of 0.01 to 0.31 mM O_2 , (c) dilution rate (h^{-1}), (d) initial amount of viable microorganisms (bacteria),
944 (e) total simulation time (h), (f) the equivalent step time (min), (g) time (h) for shutdown O_2 input flow, (h) the general
945 maintenance energy requirement ($\text{gC}_{\text{donor}}\cdot\text{gC}_{\text{mic}}^{-1}\cdot\text{h}^{-1}$), (i) the mass degradation coefficient (h^{-1}), (j) sizes for the smallest
946 and biggest microorganism (μm), (k) the coefficients for the molar relationship between the elements carbon, hydrogen,
947 oxygen and nitrogen to establish the empirical chemical formula of the denitrifying bacteria, and (l) the μ_{max} value (h^{-1})
948 as reference to establish the maximum individual uptake.

949 **6 Individual Sub models**

950 The bipartition reproduction process is a sub model that is taken from INDISIM, the generic and core bacterial model
951 (Ginovart et al., 2002). Thus, we only describe the individual sub-models that we designed particularly for the INDISIM-
952 Denitrification model.

953 **Uptake:**

954 Each nutrient uptake depends on the maximum uptake capacity of the individual to capture nutrients through the cell
955 membrane-associated proteins [13] and on the nutrient availability in the medium. Individual uptake is assumed to be
956 proportional to the individual mass and to the uptake rate (u_i being i the nutrient), which represents the amount of nutrient
957 that could be captured per unit of time, and mass ($\text{mol}_{\text{nutrient}}\cdot\text{molC}_{\text{mic}}^{-1}\cdot\text{h}^{-1}$).

958 Following the INDISIM framework (Gras et al., 2011) the maximum population growth rate (μ_{\max}) has been used to
959 estimate the maximum individual uptakes. Using this value and performing calculations with the stoichiometric
960 coefficients of each metabolic reaction adjusted by TEEM, we obtained the maximum uptake rate for each nutrient. The
961 nutrient availability (a_i) is the fraction of each nutrient (i) in a spatial cell that is accessible per unit of time (h^{-1}) and for
962 the individual. This parameter is directly related to the nutrient characteristics. In order to give values to this parameter,
963 a_i , we use Fick's law binary diffusion coefficients (D_{ab}) in water as a reference [14]. Therefore, we assumed that the
964 nutrient with maximum D_{ab} has the highest availability; the other availability values are assigned proportionally. To
965 determine the individual nutrient uptake at each time step, each bacterium compares its maximum uptake capacities with
966 the nutrient available and takes the lowest value.

967 **Maintenance:**

968 it is necessary that each bacterium achieve some energetic requirements to ensure its viability. The maintenance
969 requirements are proportional to individual's mass. Gras et al., (2011) consider an appropriate maintenance requirement
970 for soil heterotrophic microorganisms of $0.002 \text{ gC}_{\text{donor}} \cdot \text{gC}_{\text{mic}}^{-1} \cdot \text{h}^{-1}$, which was assumed for aerobic and anaerobic phases,
971 the stoichiometric coefficients are calculated according with the energy reactions (Table I).

972 When the individual carries out its maintenance, the CO_2 and the reduced e-acceptors are expelled to the culture medium
973 except the NO_2^- which is added to its corresponding intake and being able to be used in the same time step. In anaerobic
974 phase the first individual option is to accomplish the maintenance requirement carrying out the energy reaction with
975 succinate and NO_3^- ; if the bacterium cannot reach its maintenance requirements, it can try it with succinate and another
976 e-acceptor, following the reaction sequence shown in Table I.

977 After the maintenance, if the remaining succinate uptaken and the quantity of some e-acceptors are higher than zero, the
978 individual can perform individual mass synthesis.

979 **Mass synthesis and metabolic products:**

980 With the nutrient intakes updated and after the maintenance, the individual can generate its own mass following the
981 sequence reactions presented in Table II. Using the stoichiometric coefficients of each metabolic reaction (Table II). Each
982 bacterium divides the amount of each nutrient up-taken by its respective stoichiometric coefficient and selects the smallest
983 value (the limiting nutrient). This information provides the demands of each one of the nutrients, the creation of new mass
984 and metabolic products generation. The CO₂ produced is released to the culture medium and the amounts of N-oxides
985 generated are added to its corresponding intakes. After this, if there are remaining amounts of e-donor and some e-acceptor
986 intakes, the microbe can perform the next metabolic reaction.

987 **Mass degradation:**

988 if there are internal quantities of the cytotoxic gases NO and/or N₂O and the C-source quantity is not enough to execute
989 a metabolic reaction, the microbe executes the mass degradation behavior-rule. It first establishes the amount of its mass
990 that will be used to reduce internal cytotoxic products based on the mass degradation coefficient (h⁻¹), and with this
991 quantity established, the cytotoxic product is reduced following the reactions coefficients (Table III), the individual mass
992 is reduced, and the remaining unused intakes are expelled to the medium.

993 The sub models related to the bioreactor's procedure are:

994 **Agitation:**

995 Nutrients and metabolic products are redistributed in the culture medium and microorganism positions change randomly.

996 **Input flow:**

997 The bioreactor is filled with fresh medium (succinate, NH₄⁺ and NO₃⁻) with a composition equal to the initial one. A
998 dilution rate is defined as a fraction (volume) of the culture media removed and filled by unit of time.

999 **Output flow:**

1000 According to the dilution rate a fraction of the media in the bioreactor is removed and the same fraction of individuals
1001 are randomly removed.

1002 **Supplementary Material - References**

- 1003 1. Gras A, Ginovart M, Valls J, Baveye PC (2011) Individual-based modelling of carbon and nitrogen dynamics in
1004 soils: Parameterization and sensitivity analysis of microbial components. *Ecol Modell* 222:1998–2010.
1005 <https://doi.org/10.1016/j.ecolmodel.2011.03.009>
- 1006 2. Rittmann BE, McCarty PL (2001) *Environmental Biotechnology: Principles and Applications*
- 1007 3. van Verseveld HW, Boon JP, Stouthamer AH (1979) Growth yields and the efficiency of oxidative
1008 phosphorylation of *Paracoccus denitrificans* during two- (carbon) substrate-limited growth. *Arch Microbiol*
1009 121:213–223. <https://doi.org/10.1007/BF00425058>
- 1010 4. van Verseveld HW, Braster M, Boogerd FC, et al (1983) Energetic aspects of growth of *Paracoccus denitrificans*:
1011 oxygen-limitation and shift from anaerobic nitrate-limitation to aerobic succinate-limitation. *Arch Microbiol*
1012 135:229–236. <https://doi.org/10.1007/BF00414485>
- 1013 5. McCarty PL (2007) Thermodynamic electron equivalents model for bacterial yield prediction: modifications and
1014 comparative evaluations. *Biotechnol Bioeng* 97:377–388. <https://doi.org/10.1002/bit>
- 1015 6. Grimm V (1999) Ten years of individual-based modelling in ecology: what have we learned and what could we
1016 learn in the future? *Ecol Modell* 115:129–148. [https://doi.org/10.1016/S0304-3800\(98\)00188-4](https://doi.org/10.1016/S0304-3800(98)00188-4)
- 1017 7. Grimm V, Berger U, DeAngelis DL, et al (2010) The ODD protocol: A review and first update. *Ecol Modell*
1018 221:2760–2768. <https://doi.org/10.1016/j.ecolmodel.2010.08.019>
- 1019 8. Railsback SF, Grimm V (2012) *Agent-Based and Individual-Based Modeling: A Practical Introduction*. Princeton
1020 University Press
- 1021 9. Felgate H, Giannopoulos G, Sullivan MJ, et al (2012) The impact of copper, nitrate and carbon status on the
1022 emission of nitrous oxide by two species of bacteria with biochemically distinct denitrification pathways. *Environ*
1023 *Microbiol* 14:1788–800. <https://doi.org/10.1111/j.1462-2920.2012.02789.x>
- 1024 10. Schönfisch B, de Roos A (1999) Synchronous and asynchronous updating in cellular automata. *Biosystems*
1025 51:123–143. [https://doi.org/10.1016/S0303-2647\(99\)00025-8](https://doi.org/10.1016/S0303-2647(99)00025-8)
- 1026 11. Cornforth D, Green DG, Newth D (2005) Ordered asynchronous processes in multi-agent systems. *Phys D*
1027 *Nonlinear Phenom* 204:70–82. <https://doi.org/10.1016/J.PHYSD.2005.04.005>
- 1028 12. Caron-Lormier G, Humphry RW, Bohan DA, et al (2008) Asynchronous and synchronous updating in individual-
1029 based models. *Ecol Modell* 212:522–527. <https://doi.org/10.1016/J.ECOLMODEL.2007.10.049>
- 1030 13. Button DK (1998) Nutrient Uptake by Microorganisms according to Kinetic Parameters from Theory as Related
1031 to Cytoarchitecture. *Microbiol Mol Biol Rev* 62:636–645
- 1032 14. Perry R, Green D, Maloney J (1984) *Perry's chemical engineer's handbook*. McGraw-Hill Book.

1033

1034